COMPARISON OF TREE GROWTH AND RESTORATION TREATMENT PERSISTENCE IN RIPARIAN AND UPLAND CALIFORNIA MONTANE FORESTS

By

Scott David Burdette

A Thesis Presented to

The Faculty of Humboldt State University

In Partial Fulfillment of the Requirements for the Degree

Master of Science in Natural Resources: Forestry

Committee Membership

Dr. David Greene, Committee Chair

Dr. Aaron Hohl, Committee Member

Dr. Mark Rizzardi, Committee Member

Dr. Alison O'Dowd, Graduate Coordinator

May 2017

ABSTRACT

COMPARISON OF TREE GROWTH AND RESTORATION TREATMENT PERSISTENCE IN RIPARIAN AND UPLAND CALIFORNIA MONTANE FORESTS

Scott David Burdette

This thesis analyzes the growth of red fir (*Abies magnifica*) and California white fir (*Abies concolor* var. *lowiana*) in three different sites in California and creates an individual-tree, distance-independent growth simulator. The first chapter of this thesis is a literature review discussing the issues facing the forests composed of these montane true fir in California and the forest growth simulators in common use. The second chapter uses AICc model comparison to determine which models for each species best predicts growth of individual trees in terms of basal area increment (BAI). The third chapter of this thesis uses these individual-tree growth models to create a simulator from an Excel workbook to predict how long treatments would persist in uneven-aged, red and white fir composed stands. Twelve hypothetical stands were created and treated in order to illustrate treatment persistence. Sequoia National Forest (SNF) had shorter treatment persistences than similar Klamath National Forest and Tahoe National Forest (TNF) scenarios. Red fir dominated stands had shorter treatment persistences than similar white fir dominated scenarios. More moist stands had shorter treatment persistences than drier stands.

ACKNOWLEDGEMENTS

A great debt of gratitude is owed to the following individuals for help with plot establishment and measurements: Katelyn Burdette, Kathleen Kennedy, Daniel Kluegel, Christopher Kirk, Suzanne Peterson, George Powell and Rick Stevens from Sequoia National Forest, Danika Carlson and Kevin Osborne from Klamath National Forest, Chris Chase from Timber Products Company/Michigan-California Timber Company; Dr. Aaron Hohl for consultation regarding experimental design issues and solutions; George Pease for assistance with equipment procurement and expertise; Sarah Hanna for GPS data exportation assistance; and Erin Degenstein and for GIS expertise.

For assistance with project funding, the Helen Barnum family is greatly appreciated as well as the Western Regional Graduate Exchange Program.

A debt of eternal gratitude is owed to my family and friends who were constantly supportive through turbulent times during the execution of this project with specific praise to my sister, Katie Smith, and my wife, Katelyn Burdette. Without these women, this project would not have been completed.

This project is dedicated to the memories of Gayleen Smith, Cynthia Little, and Barbara Burdette; to Gayleen for the expertise of navigating collegiate bureaucracy, to Cynthia for the continuous support while determining and executing the path to a graduate education; and to my mother, Barbara Burdette, for being one of my closest friends and a wonderful mother with whom I talked almost daily about my successes and challenges while attending HSU.

TABLE OF CONTENTS

LIST OF TABLES

LIST OF FIGURES

CHAPTER 1: LITERATURE REVIEW

Introduction

The present composition of red fir (*Abies magnifica*) and white fir (*Abies concolor*) associated ecosystems are diverging from historical compositions. Both species grow fast and dense relative to other conifers in their ecosystems (Laacke & Fiske 1983, Laacke 1990a, 1990b). Both red and white fir are considered zonal climax dominant species due largely to their fast growth and shade tolerance. Both are successfully seeding into and establishing in the understory of nearby sites composed of more xeric tree communities. Historically, pine-dominated communities have been especially affected (Fites-Kaufman et al., 2007).

Both red and white fir dominated forests in California historically experienced a mixed severity fire regime where a mosaic pattern of seral and age classes was the norm (Sugihara et al. 2006). Red and white fir dominated ecosystems in California are becoming more dense and homogeneous in terms of tree species diversity due largely to a lack of active management combined with fire suppression (Fites-Kaufman et al. 2007, Fellows & Goulden 2008). Chaparral communities are also being encroached upon. Evidence exists that, although poor soil contributes to the lack of presence of these tree species within chaparral communities, historically there was a substantial component of chaparral patches in both white and red fir forests. It is estimated that fire suppression

has contributed approximately a 62% reduction in chaparral area (Fites-Kauffman et al. 2007).

In addition to their growing prevalence, individual trees of these species are highly susceptible to pathogens and infestation (Laacke 1990a, 1990b) and endure high levels of disease and damage for large portions of their lives. As climate continues to change and the boundary where precipitation occurs mainly as snow retreats upward (Maurer 2007), understanding how these species grow and interact will be critical in predicting future compositions as well as in making informed decisions regarding treatments to promote resilient stand compositions.

Red Fir

Red fir is a valuable species to study for many reasons but one of the greatest reasons is that it covers about 2% of California's total land area (Barbour & Woodward 1985). Of great significance as well, of the California forests that experience snowpack, the red fir forests of Northern California experience the greatest (Barbour et al. 1991). This is why the red fir forests of California are so important to California's water supply. Red fir is found in California, southern Oregon, and along the western border of Nevada in upper montane ecosystems. It exists fairly continuously between Kern County in the southern Sierra Nevada and Lassen National Forest in Northern California. Populations are patchy throughout the rest of its range from Lake County in the Coast Ranges of northwestern California to Mt. Shasta and as far north as approximately 44° N in the

central Cascades around Crater Lake. Other than in occasional drainages, its lower elevation limit begins around 1620 m in the Cascade and Siskiyou Mountains and increases to 2130 m in the southern Sierra Nevada. Red fir only reaches 2010 m in the Cascade and Siskiyou Mountains yet they are found at elevations up to 2740 m in the southern Sierra Nevada (Laacke 1990b, Lanner 2010). Red fir is commonly found with white fir, Jeffrey pine (*Pinus jeffreyi*), lodgepole pine (*Pinus contorta* subsp. *murrayana*), western white pine (*Pinus monticola*), sugar pine (*Pinus lambertiana*), Douglas-fir (*Pseudotsuga menziesii* var. *menziesii*), mountain hemlock (*Tsuga mertensiana*), incense cedar (*Calocedrus decurrens*), quaking aspen (*Populus tremuloides*), and regionally limited others (Laacke & Fiske 1983, Laacke 1990b, Fites-Kaufman et al. 2007).

Red fir is commonly found with infections and decay. Red fir dwarf mistletoe (*Arceuthobium abietinum* f. sp. *magnificae*) infests a large proportion of the stands in California (Cope 1993). Dwarf mistletoe-infected trees are commonly found with *Cytospora abietis*, a canker which further reduces the vigor of infected trees (Laacke 1990b). The red flagging associated with *Cytospora* canker is much more noticeable than the small mistletoe plants (Mortenson 2011/personal observation). Quantifying the effects of mistletoe-associated *Cytospora* in red fir trees is essential in order to accurately predict stand growth because biotic agents might have a stronger effect than competition (Das 2012).

The reduction of fire and logging have influenced red fir stands and associated vegetation. Red fir is largely responsible for encroaching on quaking aspen (*Populus*

tremuloides Michx.) stands, lodgepole pine (*Pinus contorta* var. *murrayana)* stands, and shrub patches. Eventual conversion to pure red fir stands occurs in the absence of high severity disturbances (Barry 1971, Chappell & Agee 1996). Considering the current amount of infection of red fir across its range and the low incidence of active management, it is apparent that red fir stands are becoming increasingly decadent (Mortenson 2011).

White Fir

White fir, with two varieties, is a common species in much of the western United States. Rocky Mountain white fir, var. *concolor*, is found between southeastern Idaho and northern Mexico. This study focuses on California white fir, var. *lowiana*, and it will be referred to as white fir throughout the report. California white fir exists in Oregon from about 600 m to about 3000 m in the San Bernadino Mountains of southern California. It extends from the Coast Ranges of Oregon throughout the southern Cascades and Sierra Nevada to Baja California (Laacke 1990a, Lanner 1999).

White fir is commonly found on more mesic sites in what is often referred to as the white fir zone (Barbour & Minnich 1988) and can exist in almost pure white fir forests (Zouhar 2001). At the upper boundary of this zone exists an ecotone between midmontane and upper montane forests where dominance transitions from white fir to red fir. The transition generally occurs over approximately 250 m of elevation and appears to correspond to the mean freezing level, the elevation at which precipitation changes from

rain to snow during storms from December to March (Barbour & Minnich 1988). White fir is also a large component of mixed conifer forests throughout California (Griffin & Critchfield 1972). It commonly exists with most of the same species as red fir but only coexists with mountain hemlock in the more northern site in this study. It also occurs with midmontane species including ponderosa pine (*Pinus ponderosa*) and giant sequoia *(Sequoiadendron giganteum),* as well as those species restricted to lower elevations including ponderosa pine, grand fir *(Abies grandis),* Pacific madrone *(Arbutus menziesii),* tanoak *(Notholithocarpus densiflorus),* and California black oak *(Quercus kelloggii)* (Zouhar 2001).

White fir has been able to increasingly dominate mixed conifer forests by seeding into the understory under intolerant conifers; the suppression of surface fires allows them to ascend into the canopy. White fir is less shade tolerant than other true firs commonly found at lower elevations, but is more tolerant than red fir and Douglas fir (Minore 1979). On xeric sites, Ponderosa pine usually dominates and associates include sugar pine, incense-cedar, and Douglas-fir. White fir is historically less common in these areas but has increased in density since the beginning of the last century (Fites-Kaufman et al. 2007). The decrease in pine reproduction from light competition, accompanied by eventual root disease and bark beetle activity, and the lack of surface fire, gradually changes the structure to more of a white fir habitat type (Lanner 1999). White fir exhibits intraspecific competition more so than interspecific competition, as is the case with most

species including red fir, except sugar pine appears to exhibit similar competition with white fir (Das 2012).

Due to fire exclusion, the landscape has advanced successionally, resulting in large areas of late successional forests with large accumulations of living and dead fuels, including ladder fuels from juvenile firs (Stephens 1998). Due to this exclusion, the likelihood of higher severity fires has increased. Therefore, white fir has great potential to influence compositions of forests both with and without fire. Without fire, the forests have become more dense than historical records suggest and, with fire, the high severity large fires that these present compositions have encouraged also leave the landscape incongruent with historical records (van Wagtendonk & Fites-Kaufman 2006).

Concerns for These Forests

Multiple concerns for these fir forests arise from current conditions and climate forecasts. The present forest compositions, which include dense stands lacking a historic mosaic quality, as well as stands with shade tolerant firs with low crowns in the understory and pines in the overstory, makes all of these stands more susceptible to fires of higher severity (Fites-Kaufman et al. 2007). Additionally, indications exist within red and white fir dominated ecosystems that the fire return intervals for historic stands were substantially shorter than previously documented due to a lack of external fire scar evidence and the ability of these trees to compartmentalize minor injuries rapidly and, conversely, rapid death and decay of trees that experience major injuries (Skinner &

Taylor 2006). Due to the incorrect notion that fire return intervals were much longer, forests with shorter fire return intervals have gained priority in terms of fuels treatments.

The lack of fire for prolonged periods of time will likely convert, or has already converted, most of these forests to high severity fire regimes from their mixed-severity regimes. Wildfires could potentially disrupt ecosystem quality and function for great periods of time by creating a more homogenous composition at large spatial scales. Additional changes would be a larger brush component including stands that would persist for long periods of time; fewer large trees for wildlife habitat; hydrophobic soils from extreme heat which would affect runoff rates; and a reduction in red fir stands that have historically maintained snowpack levels later into the summer. Plus, with climate change having more influence on extreme latitude and higher elevation ecosystems relative to those of lower and more middle latitudes (Ernakovich et al. 2014), drier and warmer or wetter and warmer conditions will likely influence the growth and succession patterns in these forests. This could also possibly position them to experience disturbances more severe than previously encountered. These disturbances could include prolonged droughts, more frequent and/or severe wind events, more influential insect outbreaks, and overall less vigorous forests which would be more susceptible to high severity wildfires and disease. A simulator designed specifically to predict density is useful given these concerns.

Without accurate growth modeling, managers could be unprepared for future conditions that would require mechanical treatments, prescribed fire, or a combination of

the two sooner rather than later to maintain stands with declining vigor or to restore a mosaic quality to these forests in order to reduce the likelihood of a disturbance that will compromise ecosystem quality and function over large areas of the landscape. Unfortunately, there are concerns with how accurately current models predict individual tree growth for these fir species in the complex forests in which they reside. This need is addressed in this research by adopting some of the dominant model parameters used by previous models and introducing other parameters that have typically been neglected, as well as testing transformations that might be better suited for these species in particular.

Growth Models and Simulators

Having the capacity to predict how forests grow over years and decades is valuable for public land managers in order to plan appropriate actions to maintain ecosystem quality and function, as well as schedule harvests. Almost all forests in California have experienced some post-European settlement disturbances, from clearcutting to overgrazing to changes to the preexisting pre-settlement fire regimes to the extirpation of keystone predators. Decisions need to be made such that, over the normal cycle of disturbance events, these forests maintain their productivity, characteristic diversity of major functional groups, and rates of biogeochemical cycling (Chapin et al. 1996). Growth models and simulators exist that predict trajectories in terms of stand densities, compositions, levels of infection, future fuel loadings, possible fire behavior, and climate change (Wensel & Biging 1988, Crookston & Dixon 2005). Being able to

determine how long a treatment will be effective is similarly important because forest managers often have limited resources for treatments. "Treatment persistence" is the time taken for thinned stands to become crowded sufficiently that competition again is intense, and is a metric that managers use to justify certain treatments. These simulators are important because, without reasonable predictions of future forest conditions, land managers could neglect to mitigate catastrophes or could even promote them.

Growth simulators are based on a collection of statistical models that predict growth of individual trees and/or stands. Simulators that predict forest growth and yield are used by both private companies and public agencies. Most growth and yield simulators are so-called 'empirical models' that were developed by fitting regressions to repeat-measures data (Taylor et al. 2009). The most common simulators used for these forests are called individual-tree/distance-independent. These simulators predict the growth of individual trees and extrapolate out to the stand scale without taking into account distance to other trees within the stand. There are also simulators that use matrix probabilities (Liang et al. 2004) as well as gap models that predict the time it takes for the area of one dominant tree to be reoccupied after it is removed (Ritchie 1999). Lastly, there are simulators that are individual-tree/distance-dependent. These simulators map trees in a stand and model their growth with factors that depend upon the size and distance to neighboring trees (Ritchie 1999).

The model in the simulator that has the most influence is called the primary driver. It is the one for which all of the other models within the simulator are based. The

primary driver for individual-tree/distance-independent simulators typically predicts diameter or cross-sectional area growth at breast height (1.4 m) from tree size, vigor, competition, site quality, and other pertinent factors for the species and stands being modeled. Simulators also use models for predictor variables of the primary driver that change as stand characteristics change. These models are considered secondary drivers and are necessary due to changes in predictor variables in the primary driver that are influenced by a dynamic system (Ritchie 1999).

Stand characteristics vary dramatically and using results from models that are not specifically designed for certain stands must be done with great caution (Smith et al. 1997). If data that were used to create growth models were collected in younger, even-aged stands that were predominantly healthy, one would be skeptical to expect the same model to perform well predicting growth in older/uneven-aged stands where many of the stand characteristics are unaccounted for. One would also be concerned if original measurements were taken during times when stands were experiencing different conditions than are occurring during the times for which simulations are run. Additionally, it is becoming an increasing concern that simulators be flexible enough to account for changes in climate and related factors that appear to be inevitable (Maurer 2007). Due to the broad range of conditions these forest ecosystems experience, having a dataset that contains the largest amount of variation possible would likely produce models that are more relevant over the ranges of conditions present and forecasted. Of particular concern is that uneven-aged stands are mandated on federal lands in California

(Troyer & Blackwell 2004). If simulators are not based on measurements from forests which have an uneven-age structure, then their reliability for use in these areas is suspect.

There are currently three publicly available simulators in use in California that overlap with both species and at least one of the sites that were used in this study. Those three include the California Conifer Timber Output Simulator (CACTOS), currently implemented under software called Forest and Stand Evaluation Environment (FORSEE) (Wensel & Biging 1988); CalPro (Liang et al. 2004); and the Forest Vegetation Simulator (FVS) (Crookston & Dixon 2005). CACTOS and CalPro were both developed using data almost exclusively from industry and private land. FVS is the dominant model in use on federal lands and is maintained by staff within the US Forest Service. All of these models have their benefits and disadvantages.

The two non-federal land based simulators are substantially different from each other. CACTOS is an individual-tree growth and yield model that uses site index, crown competition factors, and relative growth factors to model diameter growth increment of a species (Wensel & Biging 1988). This model uses data from a cooperative of timber managers from northern California and was designed for heavily managed industrial forests (Robinson & Monserud 2003). These stands are considered young-growth (Wensel et al. 1987). Since the forests in this study are mandated to be managed using uneven-aged techniques, and large size trees are retained regardless of the treatment, it would be expected that the accuracy of a simulator that predicts the growth of young stands would be suspect for accurately predicting growth of highly complex stands.

CalPro has similar problems. CalPro is a part of a family of simulators that consist of NorthPro, WestPro, and SouthPro. CalPro is specifically designed for the mixed conifer forests of California and, like its siblings, uses a site- and density-dependent matrix. This is much different from individual-tree distance independent growth simulators since it uses probabilities of: ingrowth, trees growing out of their size class, and mortality within a size. Ingrowth is the additional trees that grow into the smallest diameter class over time (Smith et al. 1997). Ingrowth is determined by stand composition, mineral soil and moisture availability, temperature, light conditions, along with numerous other biotic and abiotic factors. Mortality of trees within the size classes represented in a simulator is the naturally occurring phenomenon that takes place in forests due to density, tree size, level of infection, growth rate, level of damage, stand age, crushing, browsing, fire, along with many other natural phenomena (Reineke 1933, van Mantgem et al. 2003, Mortenson 2011). Mortality is also attributed to logging but that will be considered a treatment in this study.

Initially, parameterization of CalPro required repeat inventories and measurements of the same plots. Like CACTOS, CalPro data was collected from a collection of plots almost exclusively found on private and corporate timberlands (Liang et al. 2004). CalPro has many merits since it does model stand growth and yield well and inherently includes ingrowth and mortality. It could be a very valuable tool if it used Forest Inventory Analysis (FIA) (Bechtold & Patterson 2005) plots that included the

National Forests sampled in this study. This model type is attractive but FIA data does not include all of the variables used in this study, such as edge position and TRMI.

Finally, FVS is an individual-tree, distance-independent model that uses basal area and stand-density index (SDI) (Reineke 1933) to constrain predictions with reasonable empirical limits (Crookston & Dixon 2005). FVS is a descendent of the Prognosis Model (Stage 1973) developed for the USFS specifically for uneven-aged forest. There are twenty different geographic variants. Two variants overlap with the sites from this study. FVS predicts height and diameter growth as well as crown ratio and mortality. It also has extensions for dwarf mistletoe infection, climate change, and fire behavior. There are two different driver functions that FVS uses. The first is a height growth model for small trees and the second is a diameter growth model for large trees. Depending on the variant for a specific region, diameter growth for a specific species is predicted using terms such as tree diameter, site index, competition, elevation, aspect, slope, habitat type, crown ratio, and latitude.

It is important to ensure that whichever simulator is used to answer questions posed by managers, it is able to take into account the specific characteristics of the environment and the problem at hand. Although FVS is a very reputable simulator and represents both the areas and the species of this study, there are important characteristics of these forests that are not explicitly addressed by FVS or by the other simulators mentioned. With this in mind, a direct comparison or ranking of these simulators and the one proposed by this study is currently impossible.

The factors specifically represented in this study that pose such problems are: these forests commonly have both large and small gaps as well as fine-scale patchiness largely due to the history of mixed severity fire regime (Fites-Kaufman et al. 2007); the common presence of these species within riparian areas (Zouhar 2001); the presence of *Cytospora abieties* infection, which is a substantial contributor to decline and mortality of red fir trees throughout California; and the presence of substantial damage and disease, aside from *Cytospora,* which will be referred to as damage henceforth. Persistent damage partially includes stem wounds with visible and invisible heartwood decay; reiterated, dead and broken tops; substantial kinks; defoliated crowns; root disease; dwarf mistletoe; and bark beetles (Laacke 1990a, 1990b). A solution to these problems exists by creating a simulator that specifically addresses the stands dominated by red and white fir.

Characteristics Neglected in Existing Simulators

As mentioned previously, tree growth is sensitive to many variables, only some of which consistently appear in existing models. Since moisture availability is a critical factor for growth, it seems reasonable to include it in growth models but it is not directly used as a predictor variable in current growth models. Surrogates are used, including site index, stand aspect, and slope but they do not explicitly distinguish between riparian and upland areas, nor do they have a continuous variable for moisture availability. Site index, considered the dominant height at an indexed age, is problematic for sites that are

uneven-aged, have incurred height growth damage, have mixed species composition, or are experiencing variations in climate (Monserud 1984), As an alternative, Topographic Relative Moisture Index (TRMI) uses four different terrain-based values to create one moisture value estimate (Parker 1982). TRMI has been proven to be a valuable alternative for site index in other studies and has the potential to be of great value in these forests (Clinton et al. 1993, Beaty & Taylor 2001, Taylor & Skinner 2003).

Trees on the edges of stands, clumps, and gaps, which are common for these species in older stands, experience different growing conditions than interior trees. A couple of important characteristics of edge trees are that they experience more light and wind, and thus have lower relative humidity. Wind commonly experienced at the edges of stands in these environments can influence the way trees allocate wood to reinforce their wind-firmness (Smith et al., 1997). With respect to additional light, crown ratio is correlated to edge position through crown competition and density values found in other models (Crookston & Dixon 2005). The use of a binary edge position variable could substantially help as a surrogate for the lack of explicit positional information in distance-dependent simulators. Having an explicit variable may illustrate that the crown ratio is deceiving since the interior portion of the tree typically has fewer living branches, resulting in an inflated value for crown ratio when taking absolute crown length, as done in this study (personal observation).

In addition to these variables, species at the extremes of their niche are more susceptible to influence by additional factors than those that normally restrict growth

within the niche. In particular, competition is more influential as less favorable temperatures and moisture availability become more common for a species (Fites-Kaufman et al. 2007). This underscores the importance of species composition. Since elevation is typically considered a surrogate for temperature, interactions between species composition and elevation have the potential to be significant and should be tested. Also, under these stressful conditions, these trees may have fewer resources to compartmentalize damage and resist/defend against pathogens. Although elevation is a factor for some species in existing simulators, interactions with elevation are not included. Therefore, it seems reasonable to assume that interactions could be anticipated between elevation, as a surrogate for temperature, and other vigor-restricting factors.

Finally, with regard to climate change, having terms that can fluctuate for wetter or drier conditions as well as warmer or cooler conditions may prove to be vital. Since elevation is a surrogate for temperature and TRMI is a surrogate for moisture availability, having the ability to adjust their specific values within a simulator for these forests may be invaluable. It could have drastic effects on how long treatments last as well as the degree that competition, disease, and injury can alter the vigor of these forests.

CHAPTER 2: BASAL AREA INCREMENT MODELS OF RED FIR AND WHITE FIR TREES

Introduction

Red fir (*Abies magnifica*) and California white fir (*Abies concolor* var. *lowiana*), henceforth referred to as white fir, associated forests in California have been experiencing conditions that are of concern for forest managers. Reliably determining how long treatments will persist is an important attribute of any growth simulator that managers choose to use.

Red fir associated forests are predominantly found at higher elevations. As elevation decreases, white fir associated forests become more dominant. On more mesic sites, almost pure stands of each species exist. Within the combined elevational range, a transitional ecotone exists that is composed of an almost exclusive combination of the two species. Both red and white fir are found on less mesic sites as well. The compositions of these stands include more shade-intolerant and drought-tolerant species, such as pines. Red and white fir associated forests have been experiencing conditions that diverge from historical records as these forests transition from mixed- to high-severity fire regimes. The historical range of variation (HRV) included forests that were generally less homogeneous spatially and had somewhat different species composition. Both species thus are experiencing conditions that perhaps warrant human intervention.

In order to restore the red and white fir-dominated montane forests in California to more historical, resilient, and/or disturbance resistant conditions, forest managers need to have an understanding of how long treatments will last. In this study, this time-frame is referred to as 'treatment persistence'. There are many qualities of the trees and stands measured for this study that are neglected in existing growth simulators that might otherwise be able to predict treatment persistence. The characteristics of these tree species and associated forests that encourage the development of a novel simulator include: a clumpy structure with many trees that are on the edges of gaps and fields; the common presence of these species within riparian areas; the presence of *Cytospora abieties* infection, which is a contributor to mortality of red fir trees throughout California; and the presence of substantial damage and/or disease, aside from *Cytospora*. Persistent damage/disease partially includes stem wounds with visible and invisible heartwood decay; reiterated, dead and broken tops; substantial kinks; defoliated crowns; root disease; dwarf mistletoe; and bark beetles. Additionally, this study is conducted predominantly on federal lands where the great majority of stands have an uneven-age structure and contain many large relic trees, traits that are uncommon on non-publically owned property. A simulator that addresses these characteristics directly has the potential to be a useful tool in terms of predicting treatment persistence on federal land.

Objectives of the Study

This study looks into modeling growth in the transitional ecotone from the white fir dominated mid-montane ecosystem into the red fir dominated upper montane

ecosystem. For the first chapter, trees will be sampled across the elevational gradient in the transitional ecotone to see if a significant elevational trend is detectable by capturing the limit of the ecological niche for each species and to see if interactions with elevation and other factors, such as density and composition, are also significant. Three sites in California will be used to see if trends exist across a latitudinal gradient. Samples will be taken both within riparian areas as well as across a gradient of drier areas to see how topographic attributes that contribute to moisture availability affect growth increment. Competition composition in terms of density attributable to species will also be examined to determine if and how certain species compete, either intraspecifically or interspecifically. Finally, using the derived best BAI models, a second chapter will derive further models for predictor variables of the original BAI models that are sensitive to changing tree and stand conditions. This will simulate a variety of stands growing over decades to predict the treatment persistence of hypothetical mechanical treatments. This information gives managers at these sites, and possibly others, insight for management decisions for red and white fir stands as well as those that are a composition of the two. Hopefully, with these insights, critical stand densities where mortality is prevalent will be reduced in order to encourage more resilient stands that would better resist catastrophic wildfires and disease.

It is worthwhile to discuss the many terms that have been used in modelling growth such as size, crown ratio, competition, elevation, site quality, and infections. The terms that are unique to this study include a binary term regarding if a tree is on the edge

of an opening, a binary term representing if a tree is in a riparian area, a continuous moisture specific term called TRMI, a three level term for *Cytospora* infection, a binary term for damage, continuous terms for intraspecific and interspecific competitions, an interaction term between elevation and *Cytospora* infection, an interaction term between elevation and damage levels, and an interactions term between elevation and density.

The conventional terms mentioned previously, such as size and density, can be represented in many manners. Here, size is represented as diameter at breast height (DBH). Stand density index (SDI) and basal area (BA) were both considered in this thesis but BA does not represent density as well since it does not take into account number or size of competing trees. SDI also has well documented maximums and ranges of mortality whereas BA does not. Stand density index attributed to trees equal to and larger than the tree measured (SDIL) and basal area attributed to trees larger than the measured tree (BAL) was also measured and SDIL was chosen for similar reasons as above. Intraspecific and interspecific competition was measured in terms of the percent of SDI attributed to each species. The term for elevation is relative to the latitude and therefore it was adjusted based on the latitude of the tree sampled. Site quality was considered based on location and topographic relative moisture index (TRMI). The last conventional term is crown ratio and that was measured as the ratio of total crown length to total tree height.

Methods

Full Model

From a sample size of 131 white fir and 137 red fir, best models were determined for species specific BAI models. The full model considered includes terms for: site (Klamath National Forest (KNF), Tahoe National Forest (TNF), and Sequoia National Forest (SNF)); tree size in terms of DBH; density, either SDI or SDIL; CR, in terms of lowest live branch to the top of the tree to the total tree height or in terms of average of lowest live branches to the top of the tree to the total tree height; edge and interior stand position; level of *Cytospora* infection; two levels of damage and disease aside from *Cytospora* infection, considered less than moderate damage or more than moderate damage; the continuous term TRMI for moisture availability; a binary moisture variable, riparian vs. upland; species composition in terms of % of SDI attributed to red or white fir for intraspecific competition or interspecific competition; elevation adjusted for latitude; and interactions with elevation including elevation and damage, elevation and *Cytospora* infection, and elevation and species composition. Model determination used a priori selection criteria.

Field Methods

Climate in California is generally Mediterranean-type, having warm, dry summers and cool wet winters. Most of the moisture falls between October and April (Minnich

2007). Mountain soil moisture levels are generally better than elsewhere in the state because of the deep, longer-persisting snow pack (Fites-Kaufman et al. 2007). Elevation and aspect have an effect on vegetation type since similar vegetation will be found at different elevations on different aspects, but more importantly, soil depth and rain shadow influence moisture and can change a forest type from fir dominated to pine dominated. In this study I used sites on predominantly east facing aspects on the lee side of the crests.

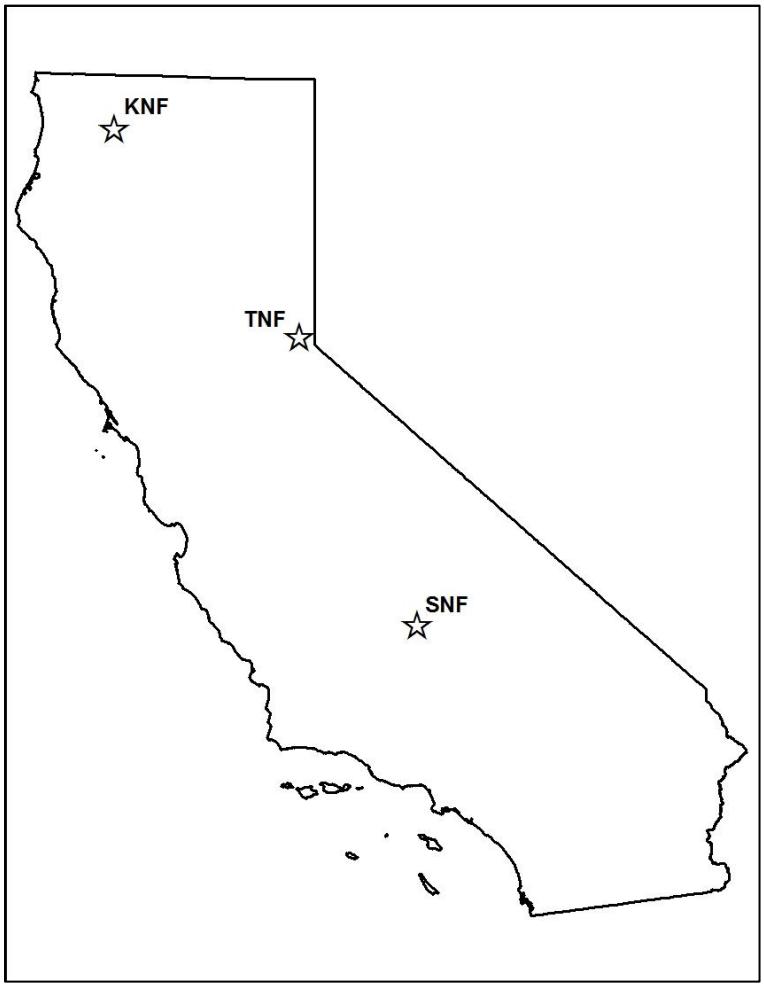

Figure 1: Locations of the three sites studied. KNF, TNF, and SNF represent Klamath National Forest, Tahoe National Forest, and Sequoia National Forest respectively. KNF includes some Timber Products Company/Michigan-California Timber Company properties.

Data were collected at three sites in montane regions of California (Figure 1; Table 1). One site was on the eastern side of the Klamath range near Etna at approximately 41.4° N latitude, 123.0° W longitude in the area of Klamath National Forest and Timber Products Company/Michigan-California Timber Company properties in the watersheds of Etna and Ruffey Creeks (KNF). A checkerboard ownership pattern

exists in this area. Average April 1st snow water content for this area over the years concurrent with growth measured, 2008 to 2012, is 66.8 cm according to the Etna Mountain snow survey report (Department of Water Resources, n.d.). Soils at KNF consist of Inceptisols ranging from shallow to very deep; these are considered well drained soils. Parent materials include basic igneous, metamorphic, and altered sedimentary rocks. Texture includes very gravelly loam, gravelly loam, and very gravelly sandy loam (Soil Survey Staff, n.d.).

The second site is in the Tahoe National Forest at approximately 39.1° latitude, -120.2° longitude in the watershed of Blackwood Creek (TNF). The nearest snow survey station is located at Lost Corner Mountain. Average April 1st snow water content during the same period was 92.2 cm (Department of Water Resources, n.d.). Soils at TNF consist of Inceptisols, Mollisols, and Andisols. The Inceptisols are very deep and very poorly drained soils from andesite and granodiorite. The texture is mucky silt loam. The Mollisols are shallow and excessively drained soils also derived from andesite with a stony fine sandy loam texture. The Andisols range from shallow to very deep and from moderately well to excessively well-drained. Parent materials are andesite and volcanic rock. Textures include gravelly and very gravelly medial course sandy loam, gravelly medial loamy coarse sand, and very cobbly ashy loam sand (Soil Survey Staff, n.d.).

The third site is in the Sequoia National Forest at 35.8° latitude, -118.6 longitude in the Bull Run Creek watershed (SNF). The nearest snow survey station that consecutively recorded data over the time period is located at Quaking Aspen

Campground. Average Aril 1st snow water content was 47.0 cm for the years associated with growth (March 2008 was substituted for April 2008 since April data were unavailable) (Department of Water Resources, n.d.). Soils at SNF consist of Mollisols, Entisols, and Inceptisols. Mollisols have deep, well drained soils from metasedimentary parent materials with a gravelly fine sandy loam texture. Entisols have moderately deep, excessively drained soils from granite parent materials with a stony course sandy loam texture. Inceptisols have soils that are moderately to very deep ranging from well to somewhat excessively drained with granite or granodiorite parent materials. The textures of these Inceptisols include coarse sandy loam and gravelly loam. All sites had extensive areas of exposed rock predominantly at the higher elevations.

Table 1: Site comparison.

Site	Location	Average April 1st snow water content (cm)	Soils
TableKNF	41.4°N, 123.0°W	66.8	Inceptisols
TNF	39.1°N, 120.2°W	92.2	Inceptisols, Mollisols, Andisols
SNF	35.8°N, 118.6°W	47.0	Inceptisols, Mollisols, Entisols

Data were collected throughout the late summer and fall of 2013. A target sampling method was used and the experimental unit was the "target tree". Target trees were chosen to represent the broadest range of conditions and tree size metrics available. Target trees were sampled along "wandering" transects across an elevation gradient, which includes the transitional ecotone between upper and mid-montane conifers. Both riparian and upland transects were used at each site. Target trees were established at least

50 m apart to partly reduce the potential for genetic relatedness. The lower size limit for target trees was 10 cm. Trees that appeared to have likely experienced major disturbances in the immediate area within the past eight years were disqualified for sampling.

Variable radius plots centered at target trees were used to estimate competition. Depending on vegetation and stand density, either an angle gauge or a wedge prism was used to determine if trees should be tallied (Avery & Burkhart 2001). The wedge prism was primarily used but an angle gauge was used when viewing the competing tree through the prism was prohibitive due to visual interference. A basal area factor (BAF) of 9.184 $m^2\ ha^{-1}$ (40 ft^2a^{-1}) was predominantly used for evaluating density of competition due to the observation that between five and twelve trees were consistently determined to be tallied for the vast majority of plots. Densities lower than 9.184 $m^2\ ha^{-1}$ were commonly missed when using this BAF. When density was consistently low across a large portion of a transect such that fewer than five trees were tallied with a 9.184 $m^2\ ha^{-1}$ BAF, a 4.592 $m^2\ ha^{-1}$ (20 ft^2a^{-1}) factor was used to produce a higher resolution of density During variable radius plot measurements, critical distances were not measured and slope was not accounted for. Instead, slope was accounted for by use of a DEM in a GIS. Due to time restrictions and the fact that the true plot center was problematic to establish since it was in the center of the target tree. Personal judgment was used to determine if borderline trees should be tallied. If two trees were considered borderline, one tree was selected for measurement. In order to compute BAL, SDI, SDIL (see Appendix for

acronyms) and proportion of BA and SDI attributed to by specific species, tallied trees were measured for DBH using a Biltmore stick and their species was recorded.

Waypoints were created for target trees in the geographic coordinate system North American Datum 1983 (NAD83) using a consumer-grade handheld GPS unit (Garmin GPSmap 60CSx). If multiple trees met target tree criteria, were within 15 m of each other, and were differing species, a single waypoint was established between them. Waypoints were established once predicted accuracy values fell below six meters in order to determine position, slope, aspect, and elevation from a geographic information system (GIS) based digital elevation model (DEM).

Target Tree Data

Once target trees were established, species was recorded. DBH (cm) was measured at 1.4 m above the uphill base using a diameter tape. Target trees were measured for radial growth using an increment borer. Radial growth for the five years between the beginning of the growing season of 2008 and the beginning of the growing season of 2013 was recorded from one increment core extracted from trees with DBH values between 10 and 20 cm and recorded from two cores for trees over 20 cm so that values could be averaged. A first core was taken on the uphill side of the tree at breast height (1.4 m). If DBH>20, a second core was taken at approximately 90^0 to the first core at the same level, typically resulting in a sidehill sample. If branches, buttressing, or damage were encountered at intended extraction locations, extractions were made at locations far enough away to avoid them but as close as practical. Displacement was

horizontal except for two red fir trees where the displacement was vertical for one by 0.4 m due to swelling and on other by -0.1 m due to branch interference. No adjustment was made for taper. Digital calipers were used and measurements were made perpendicular to ring boundaries to accurately reflect radial growth. Growth was predominantly recorded in the field. When ring boundary differentiation was difficult without magnification, a 7x magnification loupe was used. If ring differentiation was too difficult in the field, cores were measured for length and transported to the lab to have their growth measured using a microscope. Cores transported to the lab were first mounted to core boards and measured for length again to calculate percent length after shrinkage. They were then sanded with progressively finer grit sandpaper until rings boundaries were visually differentiated and growth increment was then measured with digital calipers under magnification. Values were then corrected by dividing by the proportional measure of shrinkage.

Similarly to increment core extraction locations, bark thickness was measured at breast height on the uphill side of the tree and approximately 90^0 to the first measurement for all trees. Similar adjustments were made as those for increment cores if obstacles to measuring bark thickness were encountered. Measurements were predominantly made using a bark thickness gauge. If bark thickness was greater than the maximum limit of the gauge, an increment core spoon was used at the bore holes. Depth was marked on the spoon after feeling for the hardness of wood and measured with a ruler. To reduce the error involved with local bark irregularities, external bark edge for the region of the tree

where the bark thickness was measured was estimated using the diameter tape across a portion of the circumference. Continuous live crown base height and tree height were measured using a sonic hypsometer (Haglöf Vertex IV) to calculate crown ratio (CR). Percent complete crown was visually estimated for trees that did not have complete crowns in order to estimate adjusted CR.

Target trees were deemed to be within a riparian area if flowing water was within a slope distance of 15 m. The water was considered to be perennial since observations were collected during the drier portion of the year in all sites. Strahler stream order varied from 1 to 4, most being 1 or 2. Trees were considered to be in upland areas if they did not meet these riparian criteria. Trees that had the length of their crown exposed to light from gaps on at least a full length portion were considered edge trees. Gaps are defined as areas as large as or larger than half of the local dominant tree height. Trees were considered in interior positions otherwise.

Target tree infection and damage were also recorded. Level of crown infection from mistletoe and *Cytospora* was evaluated using the Hawksworth rating system (Hawksworth 1977). Presence and severity of damage for each target tree was also recorded. Two levels were established including less than moderate damage and more than moderate damage. More than moderate damage included substantial stem wounds with visible and invisible heartwood decay; reiterated, dead, and broken tops; substantial kinks; chlorotic and defoliated crowns; weeping increment bore holes and cores that were deteriorating within the tree; and substantial evidence of bark beetle infection.

Analysis

All field data and comments were entered into Excel *(Version 2010, Microsoft corp.)* and most calculations were executed with Excel as well. Basal area increment (BAI) (cm^2) was calculated as the difference between the cross-sectional area of the tree at 1.4 m without the bark and the cross-sectional area of the tree without the bark minus five years of growth and then this value was divided by five

$$BAI = \frac{\pi\left(\left(\frac{D_1}{2}\right)^2 - \left(\frac{D_2}{2}\right)^2\right)}{5}$$

where D_1 is the diameter without bark and D_2 is the diameter without bark and without the five years of recent growth.

The individual tree metric SDI was computed for each target and each tallied tree using the individual tree formula

$$SDI_i = \left(\frac{D_i}{25}\right)^{1.6}$$

where D_i represents the DBH of the tree (Reineke, 1938; Shaw, 2005). Subsequently, SDI is used to obtain the variable plot tree expansion factor F (trees/ha)

$$F = \frac{B}{7.854 \cdot 10^{-5}\, {D_i}^2}$$

where B represents the BAF (m^2/ha) used for that plot. Note that metric SDI and standard SDI are not directly convertible because 25 mm is used as an approximation of 1 inch instead of 25.4 (Shaw 2005).

In order to estimate density correctly, slope values of 15 percent or greater must be taken into account for variable radius plots (Avery & Burkhart, 2001). Estimates of stand density associated with target trees were multiplied by the secant of the slope angle associated with the local terrain of each target tree in order to increase the accuracy of density estimations (Hodge, 1965).

$$\sum SDI_i \cdot \sec \sigma$$

where σ is the slope angle in degrees.

To derive accurate estimates of density and moisture availability, waypoints were imported into a geographic information system (GIS) software package (*ArcMAP (version 10.1, Esri)*). Waypoints were projected from the geographic coordinate system NAD83 to the projected coordinate system Universal Transverse Mercator (UTM) projection associated with NAD83. UTM zone 10N was used for KNF and TNF sites and UTM zone 11N was used for SNF. In order to derive representative estimates for terrain features for each target tree, a 15 m radius buffered area centered on each waypoint was created (henceforth referred to as buffered area). The 1/3 arcsecond resolution National Elevation Dataset (NED) (Gesch et al. 2002, Gesch 2007) digital elevation model (DEM) was used to create an elevation raster layer for each site because it was the highest resolution model publicly available for all three sites. The Spatial Analyst Extension of ArcMap was used to create raster layers for slope, plan curvature (henceforth referred to as curvature), and slope aspect (henceforth referred to as aspect) using the Slope, Curvature, and Aspect tools respectively. The Extract by Mask tool was

used to extract values from each raster layer associated with each buffered area. Elevation, slope, and aspect were extracted for buffered areas associated with all sites. Curvature was additionally extracted for buffered areas associated with upland target trees. The Zonal Statistics tool was then used to average values for each buffered area. Each value was then assigned to the associated target tree or trees associated with each waypoint. Elevation units were in meters, slope units were in degrees deviating from horizontal, aspect was in degrees azimuth, and plan curvature units were in 1/100 z-units.

The following formulas were used to transform the original GIS rendered units into TRMI units:

$5(1 - x)$ for curvature units with a range of 0 to 10,

$10.5 - \left(\frac{y}{3}\right)$ for slope units with a range of 0 to 10,

$(cos(22.5 - \alpha)) + 1) \cdot 10$ for aspect units in degrees clockwise from north with a range of 0 to 20.

TRMI position was calculated by using elevation, curvature, and slope layers as well as by creating topolines and a hillshade layer. A path was created from the ridge above the waypoint to the path of continuously flowing water below the waypoint that intersects the waypoint. The top elevation (a), the waypoint elevation (b) and the flowing water elevation (c) were recorded and then the relative position $\frac{(a-b)}{(a-c)} \cdot 20$ was calculated for position units with a range of 0 to 20.

For upland target trees, each of the four values in TRMI units was added to get a total TRMI value for each target tree (range 0 to 60). Two values were created for

riparian target trees. Riparian target trees were given the max TRMI value of 60 as per Parker (1982) and alternatively calculated with position and curvature held at their relative maximums of 20 and 10 respectively while GIS rendered values for slope and aspect were used instead of their relative maximums. This gave an alternative value for riparian target trees if the assumption that 15 m from the stream failed to be an accurate representation of riparian conditions. This alternative is TRMI.NO.RIP.

To compare target tree elevations across sites, elevations had to be adjusted to account for the transitional ecotone existing at different elevations at each site. Isotherms increase as latitudes decrease at the rate of 137 m/degree latitude (Mote 2006). The following equation was used to account for this.

$$LAT.ADJ.ELEV = E - 137(L_{Klamath} - \mathrm{L})$$

where E is elevation in meters and L is latitude in degrees and $L_{Klamath}$ is the median latitude of the target trees in KNF.

Percent competition was computed by taking the sum of SDI attributed to each species, including the target tree, and then dividing that number by the total SDI for the plot. Similarly, individual tree SDI was computed for each target tree and SDI values for trees larger than the target tree were added to the target tree SDI value to derive SDI for trees larger than the target tree (SDIL).

Statistical Analysis

Principal component analyses were conducted originally and again after best models were selected in order to see if results were more informative after

transformations were determined and categorical variables were ranked. Linear models were created and tested in R statistical software (Version 2.15.2, The R Foundation for Statistical Computing). AICc was used as the metric to identify the most predictive model and the Shapiro Wilks test was used to check for normality along with evaluation of residual plots (Faraway 2004). An a priori model selection approach was taken. The response variable (BAI) was transformed and tested using the Box-Cox function from the Mass package (Venables & Ripley 2002) in R. Predictor variables were transformed where justified by previous studies or by residual plot analyses. When models with certain transformations used on predictor variables showed lower AICc scores but an extreme amount of influence was illustrated in residual plots, those transformations were eliminated from consideration. All models in model rankings had observations with influence estimates much lower than critical Cooks distances. Bootstrapping was used to determine best error estimates for coefficients. Coefficients were bootstrap replicated 10,000 times using the function "boot" from the "Bootstrap Functions" package (Davidson & Hinkley 1997) in order to determine bias adjusted confidence intervals.

Results

Overall predictive ability of the best models are indicated by a reasonably high adjusted R-squared values (see Table 8 and Table 9). Achieving this level of predictive ability took a substantial amount of testing of combinations of variables and transformations on those variables (see Table 2 and Table 3). Choosing the best

transformation for the predictor variable DBH proved challenging. Originally, the response, BAI, was set equal to the natural log of DBH (ln(DBH)) to see which response transformation was best; henceforth "log" will be used to represent "ln" since this is the convention used in R. Log(DBH) was chosen due to repeated use by both FVS and by illustrations of best fit by Stephenson et al. (2014). The cube root transformation on the response variable (BAI) worked best for both red and white fir BAI models measured by analyzing residual plots, Shapiro-Wilks normality tests, and adjusted R-squared values. This was repeatedly tested during modeling to assure that the best response transformation remained the cube root while using an "a priori" strategy to determine the best models. The residuals vs. DBH plot was originally used without a transformation on DBH for both red and white fir. This indicated heteroscedasticity. In order to mitigate this, a quadratic transformation (DBH + DBH^2) was tested on both white fir and red fir models. The quadratic transformation improved AICc scores substantially for both. A transformation similar to the quadratic, (DBH + DBH^0.5) was also tested. The resulting AICc scores were substantially better for white fir but not for red fir. Due to this drop, as well as the additional predictor variables that appeared in the new best model when reconsidering previously disregarded predictor variables, this transformation was chosen (see Table 2, Table 3, and Figure 2).

The models that were compared for each species are indicated in Table 2 and Table 3. The model rankings are listed in Table 4 and Table 5. The coefficient estimates for the continuous variables included in the best models are displayed in Table 6 and

Table 7. The summaries of the best model are indicated in **Error! Reference source not found.**Table 8 and Table 9. And, the bootstrap summaries for the bias and adjusted error are available in Table 10 and Table 11. The best red fir model has the dummy variable DAM.MOD, where less than moderate damage is the baseline. The model also has the terms SITE and CRN.INFECT as three level factors. The baselines are SITEKNF, or KNF, and trees with no crown infection, CRN.INFECT 0. The best model for white fir has DAM.MOD and SITE terms but has EDGE.YN as a dummy variable with interior trees as the baseline.

Table 2: Red fir models tested.

Model name	Model formula
Null model	CUBE.BAI[a]~1
Model 1	CUBE.BAI~log(DBH)
Model 2	CUBE.BAI~DBH+I(DBH^2)
Model 3	CUBE.BAI~DBH+I(DBH^0.5)
Model 4	CUBE.BAI~DBH+I(DBH^2)+logit(CR)
Model 5	CUBE.BAI~DBH+I(DBH^2)+logit(CR)+SDIL
Model 6	CUBE.BAI~DBH+I(DBH^2)+logit(CR)+SDIL+SDI
Model 7	CUBE.BAI~DBH+I(DBH^2)+logit(CR)+SDIL+SITE
Model 8	CUBE.BAI~DBH+I(DBH^2)+logit(CR)+SDIL+SITE+RF.SDI
Model 9	CUBE.BAI~DBH+I(DBH^2)+logit(CR)+SDIL+SITE+EDGE.YN
Model 10	CUBE.BAI~DBH+I(DBH^2)+logit(CR)+SDIL+SITE+CRN.INFECT
Model 11	CUBE.BAI~DBH+I(DBH^2)+logit(CR)+SDIL+SITE+CRN.INFECT+DAM.MOD
Model 12	CUBE.BAI~DBH+I(DBH^2)+logit(CR)+SDIL+SITE+CRN.INFECT+DAM.MOD+LAT.ADJ.ELEV
Model 13	CUBE.BAI~DBH+I(DBH^2)+logit(CR)+SDIL+SITE+CRN.INFECT+DAM.MOD+D.R
Model 14	CUBE.BAI~DBH+I(DBH^2)+logit(CR)+SDIL+SITE+CRN.INFECT+DAM.MOD+log(TRMI.NO.DR)

Model name	Model formula
Model 15	CUBE.BAI~DBH+I(DBH^2)+logit(CR)+SDIL+SITE+CRN.INFECT+DAM.MOD+log(TRMI.NO.DR)*D.R
	CUBE.BAI~DBH+I(DBH^2)+logit(CR)+SDIL+SITE+CRN.INFECT+DAM.MOD+log(TRMI.NO.DR)*D.R+SDI+rf.SDI+EDGE.Y
Full model	N+LAT.ADJ.ELEV

a: CUBE.BAI is the cube root of BAI.

Table 3: White fir models tested.

Model name	Model formula
Null model	CUBE.BAI[a]~1
Model 1	CUBE.BAI~log(DBH)
Model 2	CUBE.BAI~DBH+I(DBH^2)
Model 3	CUBE.BAI~DBH+I(DBH^.5)
Model 4	CUBE.BAI~DBH+I(DBH^.5)+logit(CR)
Model 5	CUBE.BAI~DBH+I(DBH^.5)+logit(CR)+SDIL
Model 6	CUBE.BAI~DBH+I(DBH^.5)+logit(CR)+SDIL+SDI
Model 7	CUBE.BAI~DBH+I(DBH^.5)+logit(CR)+SDIL+SITE
Model 8	CUBE.BAI~DBH+I(DBH^.5)+logit(CR)+SDIL+SITE+WF.SDI
Model 9	CUBE.BAI~DBH+I(DBH^.5)+logit(CR)+SDIL+SITE+WF.SDI+EDGE.YN
Model 10	CUBE.BAI~DBH+I(DBH^.5)+logit(CR)+SDIL+SITE+WF.SDI+EDGE.YN+DAM.MOD
Model 11	CUBE.BAI~DBH+I(DBH^.5)+logit(CR)+SDIL+SITE+WF.SDI+EDGE.YN+DAM.MOD+LAT.ADJ.ELEV
Model 12	CUBE.BAI~DBH+I(DBH^.5)+logit(CR)+SDIL+SITE+WF.SDI+EDGE.YN+DAM.MOD+D.R
Model 13	CUBE.BAI~DBH+I(DBH^.5)+logit(CR)+SDIL+SITE+WF.SDI+EDGE.YN+DAM.MOD+TRMI.NO.DR
Model 14	CUBE.BAI~DBH+I(DBH^.5)+logit(CR)+SDIL+SITE+WF.SDI+EDGE.YN+DAM.MOD+TRMI.NO.DR*D.R

Model name	Model formula
Full model	CUBE.BAI~DBH+I(DBH^.5)+logit(CR)+SDIL+SITE+WF.SDI+EDGE.YN+DAM.MOD+TRMI.NO.DR*D.R+SDI+SITE+LAT.AD J.ELEV

a: CUBE.BAI is the cube root of BAI.

Table 4: Red fir AICc table.

Model name	Parameters	Log-likelihood	AICc	Delta AICc	Weight	Cumulative Akaike weights
Model 14	12	-74.5335	175.5831	0.0000	0.5961	0.5961
Model 15	14	-73.1072	177.6571	2.0740	0.2113	0.8075
Model 11	11	-77.8057	179.7234	4.1403	0.0752	0.8827
Model 10	10	-79.1097	179.9653	4.3823	0.0666	0.9493
Model 13	12	-77.7836	182.0833	6.5002	0.0231	0.9724
Model 12	12	-77.7915	182.0991	6.5161	0.0229	0.9954
Full model	18	-71.7476	185.2917	9.7087	0.0046	1.0000
Model 7	8	-93.9156	204.9562	29.3732	0.0000	1.0000
Model 8	9	-93.2937	206.0046	30.4216	0.0000	1.0000
Model 9	9	-93.3903	206.1979	30.6148	0.0000	1.0000
Model 5	6	-100.6539	213.9539	38.3708	0.0000	1.0000
Model 6	7	-99.9657	214.7995	39.2165	0.0000	1.0000
Model 4	5	-104.0741	218.6062	43.0231	0.0000	1.0000
Model 2	4	-131.7496	271.8022	96.2191	0.0000	1.0000
Model 3	4	-132.0772	272.4575	96.8744	0.0000	1.0000
Model 1	3	-134.2164	274.6132	99.0301	0.0000	1.0000
Null model	2	-193.1709	390.4313	214.8482	0.0000	1.0000

Table 5 White fir AICc table.

Model name	Parameters	Log-likelihood	AICc	Delta AICc	Weight	Cumulative Akaike weights
Model 13	12	-61.9925	150.6291	0	0.412	0.412
Model 12	12	-62.6213	151.8868	1.2576	0.2197	0.6318
Model 10	11	-64.2058	152.63	2.0009	0.1515	0.7833
Model 11	12	-63.5682	153.7805	3.1514	0.0852	0.8685
Model 14	14	-61.4886	154.5979	3.9688	0.0566	0.9251
Model 9	10	-66.4457	154.7248	4.0957	0.0532	0.9783
Model 8	9	-69.0811	157.6498	7.0207	0.0123	0.9906
Full model	16	-61.1694	159.1107	8.4816	0.0059	0.9966
Model 7	8	-71.6884	160.5572	9.9281	0.0029	0.9994
Model 5	6	-75.9311	164.5396	13.9105	0.0004	0.9998
Model 6	7	-75.63	166.1705	15.5414	0.0002	1
Model 4	5	-81.8227	174.1254	23.4963	0	1
Model 3	4	-115.5786	239.4746	88.8455	0	1
Model 2	4	-119.3518	247.0211	96.3919	0	1
Model 1	3	-124.0478	254.2846	103.6555	0	1
Null model	2	-179.1663	362.4264	211.7973	0	1

Table 6: Statistics for continuous terms in best red fir models.

Term	Min	Median	Mean	Max
BAI (cm^2)	0.97	25.07	34.73	158.20
DBH (cm)	10.2	35.2	43.3	134.8
CR	0.2698	0.7444	0.7055	0.9328
SDIL	66.0	510.4	625.1	2264.0
TRMI.NO.DR	7.707	38.770	37.090	54.300

Table 7: Statistics for continuous variables in best white fir model.

Term	Min	Median	Mean	Max
BAI (cm^2)	0.76	24.01	28.66	113.5
DBH (cm)	10	32.2	43.9	161.4
CR	0.304	0.7222	0.6993	0.9521
SDIL	90.9	632.6	698.6	2286
TRMI.NO.DR	5.286	38.77	37.45	54.83
WF.SDI	0.184	0.805	0.771	1

Table 8: R summary of best red fir basal area increment (BAI) model coefficients. The model is represented by the formula: BAI ^1/3~ DBH + DBH^2 + logit(CR) + SDIL + SITE + CRN.INFECT + DAM.MOD + log(TRMI.NO.DR). (Residual standard error: 0.4347 on 126 degrees of freedom, Multiple R-squared: 0.8231, Adjusted R-squared: 0.809, F-statistic: 58.61 on 10 and 126 DF, p-value: < 2.2e-1)

Coefficients	Estimate	Std. Error	t value	Pr(>|t|)	
(Intercept)	1.20E-01	4.58E-01	0.262	0.793874	[a]
DBH	6.62E-02	5.28E-03	12.552	< 2e-16	***
I(DBH^2)	-3.70E-04	4.11E-05	-9.003	2.87E-15	***
logit(CR)	3.34E-01	5.68E-02	5.876	3.51E-08	***
SDIL	-4.74E-04	1.18E-04	-4.005	0.000105	***
SITESNF	2.38E-01	1.14E-01	2.087	0.038911	*
SITETNF	-1.80E-01	9.35E-02	-1.921	0.056965	.
CRN.INFECT1	-2.08E-01	1.03E-01	-2.023	0.04518	*
CRN.INFECT2	-7.19E-01	1.52E-01	-4.729	5.95E-06	***
DAM.MOD	-2.13E-01	1.13E-01	-1.883	0.062024	.
log(TRMI.NO.DR)	2.93E-01	1.18E-01	2.483	0.014344	*

a : Signifiance codes: 0 ‘***’ 0.001 ‘**’ 0.01 ‘*’ 0.05 ‘.’ 0.1 ‘ ’ 1

Table 9: R summary of best white fir basal area increment (BAI) model coefficients. The model is represented by the formula: BAI^1/3 ~ DBH + DBH^0.5 + logit(CR) + SDIL + SITE + WF.SDI + EDGE.YN + DAM.MOD + TRMI.NO.DR. (Residual standard error: 0.4058 on 120 degrees of freedom, Multiple R-squared: 0.8329, Adjusted R-squared: 0.8189, F-statistic: 59.8 on 10 and 120 DF, p-value: < 2.2e-16)

Coefficients	Estimate	Std. Error	t value	Pr(>|t|)	
(Intercept)	-1.68E+00	4.08E-01	-4.11	7.27E-05	***[a]
DBH	-5.81E-02	6.65E-03	-8.738	1.70E-14	***
I(DBH^0.5)	1.09E+00	9.65E-02	11.329	< 2e-16	***
logit(CR)	2.94E-01	5.60E-02	5.246	6.77E-07	***
SDIL	-4.44E-04	1.06E-04	-4.175	5.68E-05	***
SITESNF	2.97E-01	9.91E-02	3	0.00329	**
SITETNF	1.54E-01	9.45E-02	1.631	0.10553	
WF.SDI	-3.97E-01	1.54E-01	-2.578	0.01116	*
EDGE.YN	1.76E-01	9.18E-02	1.916	0.05769	.
DAM.MOD	-2.07E-01	1.08E-01	-1.908	0.05873	.
TRMI.NO.DR	8.77E-03	4.32E-03	2.031	0.04449	*

a : Signifiance codes: 0 ‘***’ 0.001 ‘**’ 0.01 ‘*’ 0.05 ‘.’ 0.1 ‘ ’ 1

Table 10: Ordinary nonparametric bootstrap statistics with 10,000 replications for red fir BAI model coefficients.

Coefficients	Original	Bias	Adjusted confidence interval
Intercept	0.119800805	6.23E-03	(-0.7895, 1.0620)
DBH	0.066217113	1.66E-04	(0.0548, 0.0761)
I(DBH^2)	1	—	(— , —)
logit(CR)	0.3334626	1.33E-03	(0.2158, 0.4420)
SDIL	-0.000473662	1.21E-06	(-0.0007, -0.0002)
SITESNF	0.237933326	-4.26E-03	(0.0225, 0.4569)
SITETNF	-0.179602636	8.23E-03	(-0.3773, -0.0138)
CRN.INFECT1	-0.208190401	4.92E-03	(-0.4389, 0.0157)
CRN.INFECT2	-0.718890889	-1.23E-03	(-1.0852, -0.3867)
DAM.MOD	-0.212783671	7.70E-04	(-0.4326, -0.0131)
log(TRMI.NO.DR)	0.292604124	-5.05E-03	(0.0416, 0.5160)

Table 11: Ordinary nonparametric bootstrap statistics with 10,000 replications for white fir BAI model coefficients.

Coefficients	Original	Bias	Adjusted confidence interval
Intercept	-1.677100663	-3.56E-02	(-2.486, -0.870)
DBH	-0.058087618	-1.26E-03	(-0.0736, -0.0410)
I(DBH^0.5)	1	—	(— , —)
logit(CR)	0.293966023	-1.22E-03	(0.1770, 0.4116)
SDIL	-0.000443623	-4.69E-06	(-0.0006, -0.0002)
SITESNF	0.297275069	8.34E-03	(0.0942, 0.5011)
SITETNF	0.154130866	3.44E-03	(-0.0284, 0.3303)
WF.SDI	-0.397296714	-4.84E-04	(-0.7151, -0.1013)
EDGE.YN	0.175832752	-4.17E-03	(-0.0183, 0.3686)
DAM.MOD	-0.20694634	6.16E-03	(-0.4511, 0.0308)
TRMI.NO.DR	0.008767256	-2.21E-04	(0.0013, 0.0174)

Figures 2 through 10 indicate how individual predictor variables behaved across the ranges measured for both species with respect to BAI. All other variables were held at constant values. These values were the average of the medians for each species so that comparison would be considered as if trees were grown under identical conditions. Figures 2 through 5 indicate how categorical predictor variables influence DBH trends. Figure 6 illustrates how healthy red fir trees compare to healthy white fir trees. Trees on edges and interior are taken into consideration for white fir because this variable was not incorporated into the best model for red fir and it is assumed to be a representation of a combination of both.

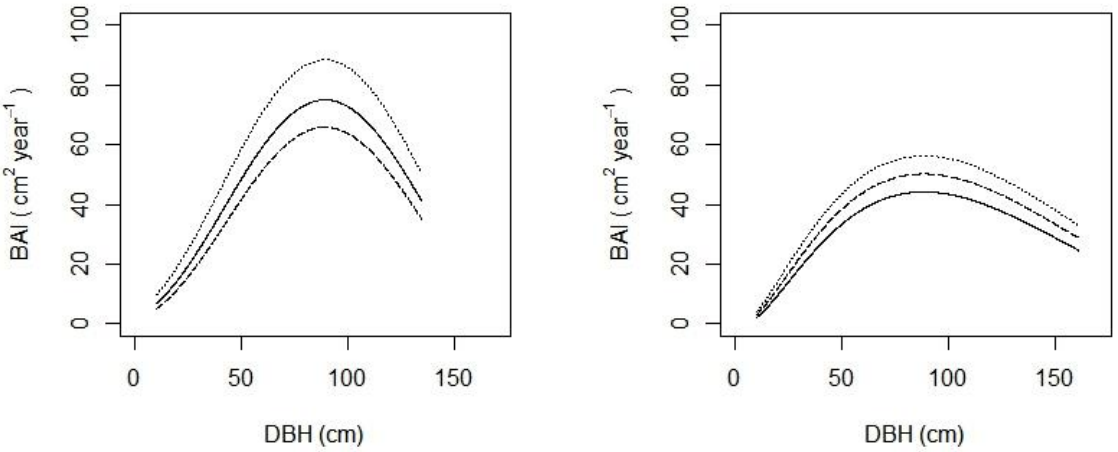

Figure 2: BAI as a function of diameter at breast height (DBH) with Klamath solid, Sequoia dotted, and Tahoe dashed. Red fir is on the left and white fir is on the right. All continuous variables are averages of the medians of both species, damage=0 for both species, crown infection=0 for red fir, and position=interior for white fir.

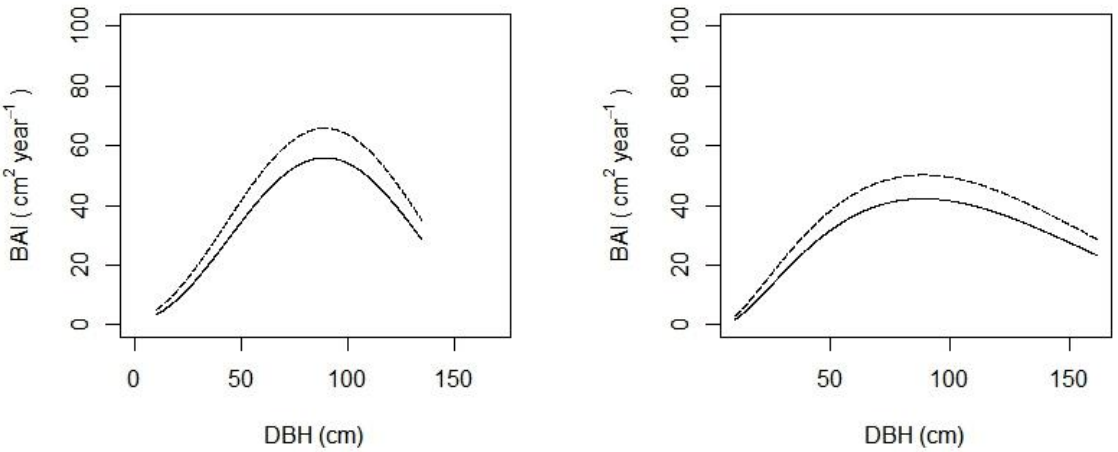

Figure 3: BAI as a function of DBH with undamaged dashed and damaged solid. Red fir is on the left and white fir is on the right. All continuous variables are averages of the medians of both species, site = Tahoe for both species, crown infection=0 for red fir, and position=interior for white fir.

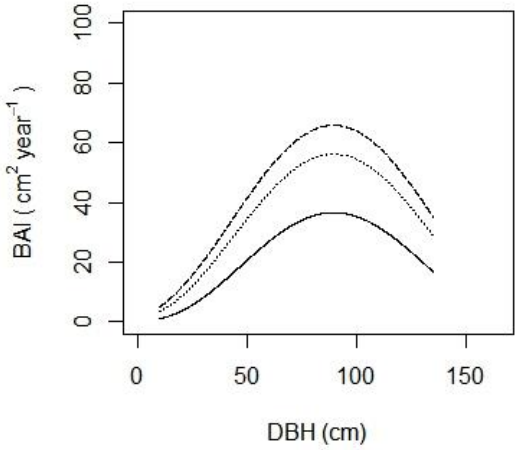

Figure 4: BAI as a function of DBH for red fir with crown infection=0 dashed, crown infection=1 dotted, and crown infection=2 solid. All continuous variables are averages of the medians of both species, the site is Tahoe, and damage=0.

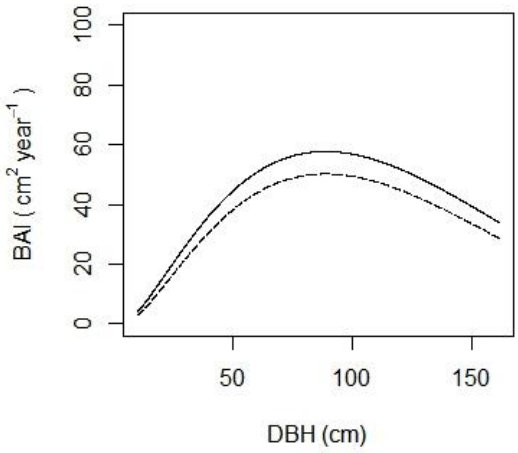

Figure 5: BAI as a function of DBH for white fir with position=edge solid and position=interior dashed. All continuous variables are averages of the medians of both species, the site is Tahoe, and damage=0.

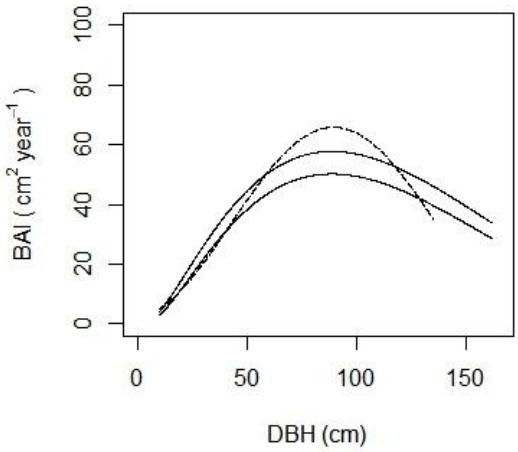

Figure 6: BAI as a function of DBH comparing red fir and white fir. The dashed line is red fir and the solid lines are white fir, with the top solid line indicating edge position and the bottom solid line indicating interior. All other values are the average of medians, the site is Tahoe, damage=0 and CRN.INFECT = 0 for red fir.

Variables that occurred simultaneously in best models for both species included crown ratio (CR), SDIL (stand density attributable to trees larger than the target tree), the binary variable for moderate or less damage vs. greater than moderate damage, the categorical variable for SITE, and TRMI.NO.DR (the variable for TRMI without a riparian default) (Table 8 and Table 9).

Crown ratio (CR) was added after DBH since it is widely considered a measure of tree vigor. The logit transformation was taken due to the limit between 0 and 1 (Warton & Hui, 2011) (Figure 7). Comparing Figures 6 and 7 illustrates that only a narrow range of values for CR are more influential on growth than DBH.

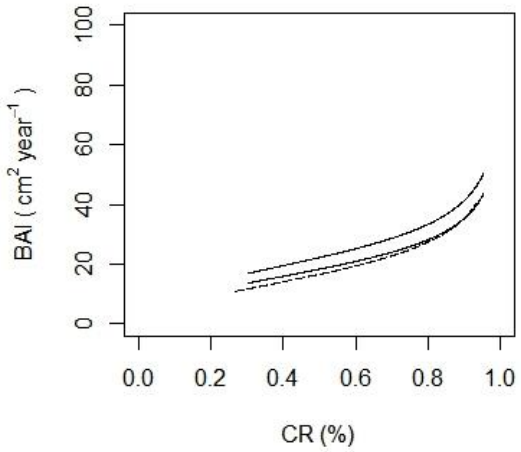

Figure 7: BAI as a function of crown ratio (CR) comparing red fir and white fir. The dashed line is red fir and the solid lines are white fir, with the top solid line indicating edge position and the bottom solid line indicating interior. All other values are the average of medians, the site is Tahoe, damage=0 and CRN.INFECT = 0 for red fir.

A competition metric was tested next and the value that best predicts BAI was stand density attributable to trees larger than the target tree (SDIL). When SDIL and SDI were tested, SDIL alone best improved AICc ranking (Table 4 and Table 5). A further look into why SDIL was a better predictor for both species resulted in a comparison of the variance inflation factor (VIF) for both terms using the "faraway" package for R (Faraway, 2004). The VIF for CR increased when SDI was only included and the VIF for DBH increased when SDIL was only included. This illustrates a correlation between CR and SDI and a correlation between DBH and SDIL. Trends for both species are illustrated in Figure 8. Comparing Figures 6 and 8 illustrate how DBH is a much greater predictor for BAI than SDIL except for at the lower values of SDIL and DBH

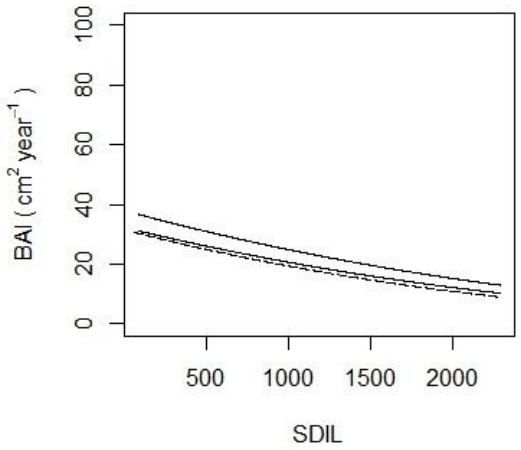

Figure 8: BAI as a function of stand density index larger that the target tree (SDIL), including the SDI value attributed to the target tree, comparing red fir and white fir. The dashed line is red fir and the solid lines are white fir, with the top solid line indicating edge position and the bottom solid line indicating interior. All other values are the average of medians, the site is Tahoe, damage=0 and CRN.INFECT = 0 for red fir.

Many of the trees associated with moderate or greater damage for both species had high influence (approximately 0.2). Therefore, a greater degree of coefficient and model accuracy would have likely occurred if more observations with moderate or greater damage were recorded but observations related to trees with this condition were well within Cook's distance when plotted on influence vs. outlier residuals graphs. The results of a damage term in the best models are illustrated in Table 8 and Table 9 and Figure 3.

TRMI.NO.DR was common in both best models but a log transformation improved AICc ranking for the red fir models whereas it did not for the white fir models. Figure 9 illustrates how BAI dips at the beginning and end of the scale of TRMI for red

fir compared to white fir. It also illustrates that white fir is more sensitive to moisture content.

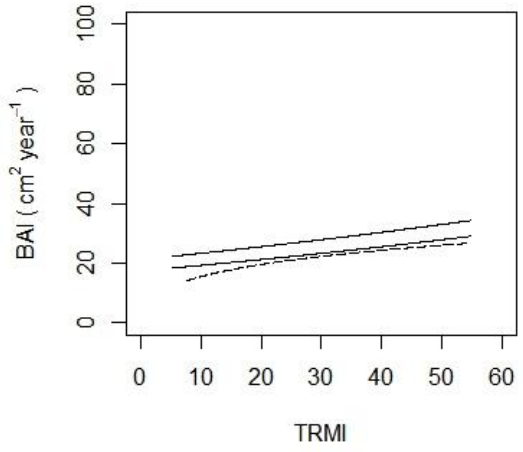

Figure 9: BAI as a function of topographic relative moisture index (TRMI) comparing red fir and white fir. The dashed line is red fir and the solid lines are white fir, with the top solid line indicating edge position and the bottom solid line indicating interior. All other values are the average of medians, the site is Tahoe, damage=0 and CRN.INFECT = 0 for red fir.

Differences between the best models for the two species were seen for the following terms: intraspecific competition, edge vs. interior, and crown infection. Intraspecific competition was tested for both species but only helped AICc ranking for white fir (Table 5, Table 9 and Figure 10). Since the coefficient was negative, this indicates that additional SDI attributable to white fir reduces how well white fir grows. Unlike using a logit transformation for CR, using a logit transformation for WF.SDI was inapplicable due to observations having exclusively white fir competition, i.e., WF.SDI = 1. This condition results in these observations having a logit transformed value of positive infinity and makes them unavailable for statistical analysis.

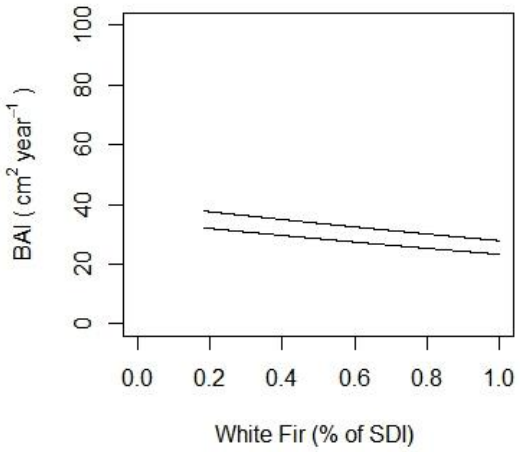

Figure 10: BAI as a function of percent of SDI attributable to white fir. The top line is white fir indicates edge position and the bottom line indicates interior. All other values are the average of medians, the site=Tahoe and damage=0.

White fir edge position showed an increase in AICc ranking whereas it did not in red fir (Table 4 and Table 5). Figure 5 illustrates how much of an influence it has when combined with the trend for DBH. Comparing Figure 9 and Table 9 illustrate that edge position is effectively equivalent in influence to damage.

Observations for trees with crown infections were substantially more common in red fir (n=36) than in white fir (n=8). These white fir observations also had disproportionately high levels of influence when residuals were plotted for models that contained the variable. Due to this, crown infection was excluded as a potential predictor variable for white fir BAI models. How BAI responds to crown infection is represented in Table 8 and Figure 4.

Principal component analyses (PCA) was conducted with variables transformed and ordered according to linear modeling results and few additional insights were found. For red fir, when the first two principal components were set as predictor variables for cube root transformed BAI, each showed little correlation. To illustrate, the third principal component for red fir, which could be interpreted to be related to size (Figure 11) was moderately correlated with CUBE.BAI as indicated by a R-squared value of 0.3871. By comparison, when CUBE.BAI was modeled with only the predictor variable log(DBH), the R^2 value was 0.5771. Ultimately, the PCA failed to assist with model selection but rather illustrated how strongly correlated the predictor variables are.

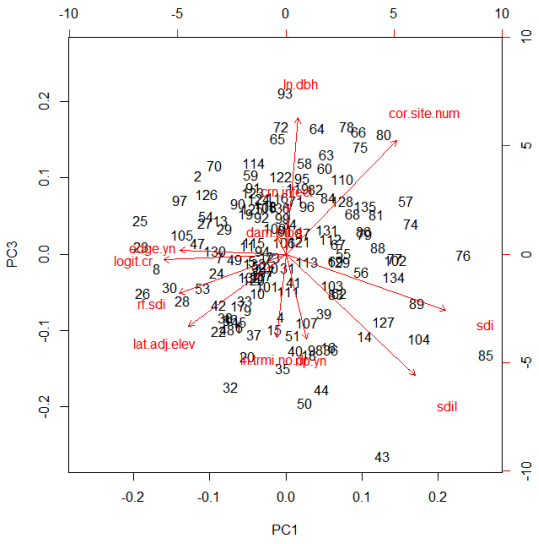

Figure 11: Principal components 1 and 3 of red fir predictor variables illustrating how PC3 can be considered correlated with size and PC1 can be considered correlated with density but variables are not clearly aligned with either.

Discussion

Multiple variables that were expected to appear in the best models failed to do so. Although elevation was originally expected to be a significant variable as a surrogate for temperature, it failed to do so. Significant interactions were also expected to be found with elevation but this also failed. The upland vs. riparian variable (D.R) was also expected to be present in the best model but this variable did not help AICc ranking for either species. An interaction term with D.R and TRMI.NO.DR was tested in order to see if riparian values amplified BAI or dampened BAI. Although this interaction did show up in some of the best red fir models, it did not show up in the final model. It has been suggested that high moisture levels found in meadows can restrict red fir growth (Laacke, 1990b) but this was not found to be apparent in this study. A quadratic TRMI.NO.DR transformation was also tested in order to see if values at the upper end of the TRMI.NO.DR scale dipped due to soil saturation and a more anaerobic conditions but this produced a lower AICc ranking.

A principal component analysis showed that size and competition were generally the most influential predictors. Ultimately the analysis did not produce a best model although it illustrated that the majority of the variables tested are highly confounded. This is also illustrated by the changes in variance inflation factors (VIF) when comparing DBH, CR, SDI, and SDL. During preliminary model analysis, SDI and SDIL were highly correlated and both could not be represented directly in the best models. When a model was tested with DBH, CR, and SDI, the VIFs were greater for CR and SDI than

for DBH. When DBH, CR, and SDIL were tested, VIFs for DBH and SDIL were greater than for CR. This might indicate that SDI is more correlated with CR but SDIL is more correlated with BAI. This does indicate that SDIL is a better direct predictor for BAI but SDI is likely represented indirectly through CR.

A quadratic transformation was chosen for DBH in red fir and a binomial transformation that included a square root term instead of a squared term was used for white fir. Although log is used as a common transformation for DBH, these transformations were substantially better and supported by the use of both a log term and a squared term by FVS (Keyser 2008). An additional negative coefficient indicates that beyond a certain size, growth decreases. This might be an artifact of the study design since many of the trees that were very large were substantially larger than the surrounding trees, which is why they were selected, and should be categorized as emergent (Smith et al. 1997). These trees may be allocating more resources to other parts of the tree than to growth at breast height. One consideration is that they are possibly allocating more resources to compartmentalize internal decay. These trees are likely substantially older than the neighboring trees and these true fir species are notorious for heart rots and root diseases (Laacke, 1990a, 1990b), which, along with fir engraver beetle, were not included in the metric for damage. Roots in these trees are largely understudied and they may be also allocating more to roots than for xylem within the bole at breast height. Likewise, there may be an element of underground competition that is not accounted for with the greater size of these trees. These species are known to root

graft and smaller trees may be taking advantage of these larger trees. "Living stumps" were repeatedly encountered while collecting data. These are stumps from trees that were cut and the cambia continued to grow as a response to heal the wound although the tree obviously had no photosynthesizing capability. These large trees may be supporting this compartmentalization more than smaller trees. If this study were to be repeated, it is recommended that observations be recorded for basal damage and any sign of conks in order to see if, after taking these damage vectors into account, BAI continues to grow logarithmically or if they continue to grow quadratically.

Crown ratio and competition (SDIL) were both expected to have significance in the best models and this was the case. The transformations chosen indicate that values at the extremes of the ranges of the terms have disproportionate influence than in the center of the range. These two terms are also correlated since low density competition gives the trees more room and light and a greater ability to retain branches that provide more than self-sustaining respiration.

As mentioned previously, intraspecific competition has been seen in white fir and it was also indicated in this study in the form of a negative coefficient for the term WF.SDI. Red fir models also showed this trend but, unlike for white fir, the term did not end up in the best model. White fir is one of the more shade tolerant conifer species and is more shade tolerant than red fir. White fir has a lower recorded maximum SDI than red fir, 1900 and 2500 SDI respectively, when grown in even aged pure white fir stands (Reineke 1938), But it was regularly found to exist in higher densities when not

competing exclusively with white fir in the uneven aged stands in this study. There were six observations where the SDI was greater than 2000 and two of those were composed of over 87% white fir. The maximum value observed for a mixed observation was 2370 and it was 69% white fir. Of these observations, the maximum SDI attributable to white fir within the composition was 2000. The maximum SDI value for a pure white fir observation was 1907. Observed maximum red fir densities were similar to published maximums, 2516 and 2514 were the greatest observations. From these few observations, the maximum SDI attributable to white fir in a mixed stand is not substantially larger than when it is in a pure stand. It appears that white fir is able to take advantage of resources that other species are not when it is in a mixed stand but they still cannot greatly exceed their exclusive maximum SDI when pure. There could also be some error involved since SDI values were increased relative to the slope. SDI might also been a better variable if trees smaller than 10cm were used to account for total competition.

It is not surprising that SITE showed up as a significant predictor variable for these species. In particular, red fir varies by site. Three varieties exist for red fir; var. *magnifica*, var. *shastensis* and var. *Critchfieldii* that correspond to KNF, TNF, and SNF respectively. It is safe to assume that substantial genetic differences within the white fir variety *lowiana* exist between the sites as well. Other reasons that site is a valuable predictor is likely due to the fact that soil composition changes at each site. Soil was generally deeper at the Sequoia site, especially at higher elevations compared to the other two sites. A bit surprising was the observation that the order of the level of influence of

the sites on BAI was not consistent between the two species. For white fir, the order from least to greatest coefficient ranking was KNF, TNF, then SNF. For red fir, the order was TNF, KNF, then SNF. As mentioned, the soil at Sequoia was deeper but the reasons why the other two were inconsistent await further inquiry. Examination of the bootstrap-adjusted confidence intervals (Table 11) indicates that for white fir, KNF and TNF intervals overlap. Therefore, it is reasonable to consider the two effectively equivalent and the ordering possibly the same as for red fir.

White fir edge position shows an increase in AICc ranking whereas it does not in red fir. It is hard to postulate why this might be the case. The median crown ratio values were very similar at 74% and 72% for white fir and red fir respectively and the number of edge trees were also similar at 42 and 52. Live branches were imagined to be repositioned up and around to fill in the spaces missing branches and values were recorded for absolute lowest live branch. Trees on edges of openings had larger crown ratios using the latter technique due to their longer crowns on the edgeward side. Although values for both techniques were recorded, the metric in this study used the latter technique since modeling indicated that it improved the AICc ranking for white fir substantially more than the former did for red fir. The median values for the former technique of adjusting crown ratios were effectively identical for each species at 63% each. It is hard to imagine that CR accounts substantially more for edge position in red fir than in white fir and would negate the presence of an edge term in the best model. It

appears that other reasons must exist for white fir benefiting from being on the edge, such as a reduction in intraspecific competition.

Damage variables were significant and negative for both species. This is likely due to the resources being diverted for compartmentalizing damage instead of investing in radial growth. Similarly, crown infection can be fatal for trees and a reduction in resource allocation at breast height is reasonable. Red fir trees with crown infection values of 2 grew much more slowly than trees with values of zero or one. Trees with substantial damage and crown infection values of 2 are likely highly susceptible to mortality due to their lower growth rates (van Mantgem et al. 2003).

As seen lately in California, metrics that independently account for moisture availability should be considered paramount in the creation of an accurate model. Moisture availability generally surpasses altitude as a driver of niche quality (Fites-Kaufman et al. 2007) and, as such, it should be expected that moisture availability would be more significant, which was true in terms of both red and white fir AICc rankings since altitude did not make it into the best models. Both red fir and white fir benefit from increasing moisture (Chapter 2, Figure 9). White fir appears to benefit slightly more and the log transformation on the red fir variable does not drastically differentiate the trajectory between the two. Red fir apparently does more poorly on dry sites and extremely wet sites compared to white fir. This likely relates to the soil and snow conditions typically experienced by red fir. This species has a greater tendency to experience a pulse of moisture availability at the beginning of the growing period when

the snow begins to melt; there will be far less available moisture throughout the summer due to the typically shallower and well drained soils. By contrast, white fir generally exist on lower slopes and in deeper soils that have moisture available longer throughout the growing season. Additionally, white fir exists on many xeric sites throughout the western United States whereas red fir is generally limited to more mesic sites (Fites-Kaufman et al. 2007). In order to calibrate this relative metric, additional studies are necessary.

In summary, the best model for red fir included terms for size (DBH), photosynthetic ability (CR), competition (SDIL), site, damage, moisture availability, and crown infection. The best white fir model includes these same terms (except for crown infection) as well as an intraspecific competition term and a term for edge position. These differences might be due to of the small sample size. These models should complement previous models regarding these montane true firs in California. Perhaps the greatest benefit of these models is that they are largely dependent upon SDI values, which are most pertinent when mortality is imminent (60% of maximum SDI) and a maximum density exists.

Limitations of the Study

Density contributed from trees smaller than 10 cm was discarded because it was determined that the values were inflated when using variable radius plot measurements. Fixed area plots would have solved this problem but revisiting the trees was impossible since they were not monumented. Therefore, SDI measurements are not as accurate as preferred. Also, density measurements were made with angle gauges and prisms without

accounting for slope in the field. The mathematical correction for this assumes that the species composition of the corrected competition level is similar to the composition of the original measurement. Further inquiry into these assumptions is warranted.

CHAPTER 3: COMPARISON OF STAND GROWTH AND TREATMENT PERSISTENCE

Introduction

The purpose of this chapter is to create a simulator to implement the basal area increment (BAI) growth models developed for red fir and white fir from Chapter 2 and to determine treatment persistence. These models are individual-tree/distance-independent models. Since the white fir model has a term that indicates whether or not the tree exists on the edge of a gap or a clearing, it may be considered semi-distance independent but that category of simulator has yet to be established. These BAI models are considered primary driver functions.

A Microsoft Excel (Excel version 2010) workbook was used to implement the models and create a growth simulator. In addition to implementing the models for growth, accounting for mortality and ingrowth was needed. Functions were created that could be adjusted by the user to help predict both.

The workbook produced predicts growth over fifty-five years. This workbook accommodates a treatment, determined by the user, and produces a graph that illustrates stand growth and treatment persistence using SDI as the density metric (see the definition of terms section at the end of this chapter for abbreviations). It also keeps track of WF.SDI so that the user can see how the SDI composition changes over time. In order to illustrate how the workbook works, twelve stands were created. These stands start with approximately the same number of trees and the same SDI but consist of two different WF.SDI compositions, two different LAT.ADJ.ELEV values related to the different WF.SDI compositions since white fir is

generally more dominant at lower elevations, three sites, and two different levels of moisture availability in terms of TRMI.NO.DR. Similar treatments were done to each stand.

Methods

To implement the two BAI driver functions, two additional models were created for each, resulting in a total of 6 models. Of the predictor terms included in the BAI models, an additional model needed to be created to describe how the CR of individual trees change as the stand changes. Additionally, a term for height to diameter ratio (HT.DBH) in m/cm was determined to be a significant predictor variable for these CR models. Models needed to be created for these HT.DBH variables as well since their values also change as stand conditions change.

As with CR and HT.DBH, some variables are dependent upon the growth from the past year while others are not. The variables that are independent of the previous year's growth and are related to site qualities include the variables SITE, LAT.ADJ.ELEV, and the continuous variable TRMI.NO.DR. Other variables that are also independent of the previous year's growth depend upon the condition of the tree or the position of the tree in the stand. These include categorical variables CRN.INFECT, DAM.MOD, and EDGE.YN. The remaining variables that are dependent upon the previous year's growth include DBH, CR, SDIL, and WF.SDI. These variables are recalculated each year based on the conditions of the previous year. In addition to implementing the models for growth, accounting for mortality, ingrowth, and treatments was needed.

An Excel workbook was created to simulate a single hectare stand growing and to determine treatment persistence. The Visual Basic Add-In was used to implement functions. The functions include the best models for BAI, CR, and HT.DBH for both species. Functions for LAT.ADJ.ELEV, TRMI slope, TRMI aspect, TRMI position, individual tree SDI, diameter increment (DI), ingrowth, mortality, and diameter distribution were also created and implemented with Visual Basic. The best models for CR and HT:DBH were determined using similar methods as those used to determine BAI models from Chapter 2. The same Chapter 2 terms were tested for both models and included HT:DBH for CR. AICc was the metric used to determine the best model for each of the four response terms. After determining the best models, bootstrapping with 10,000 replications was used to determine estimations of bias and improve estimations of standard errors.

Using the data collected, a diameter distribution was created that represented a single hectare stand found in one of these forests. Diameter distributions for most naturally occurring stands are typically represented by an "inverse J-shaped" distribution (Moser 1976). The chi-squared distribution with two degrees of freedom (k = 2) was used in order to produce an exponential function where the user determines the initial number of trees in the smallest diameter class. The tree distribution worksheet was divided into 10 cm diameter classes starting at 10 cm and each class is represented as the middle of the diameter class. For example, the first diameter class is from 10 to 20 cm and is represented by 15 cm. This is the initial diameter of all trees in this diameter class. The formula used is $DDist = TPDfifteen \times e^{\left(\frac{(15 - DCLASS)}{22}\right)}$, where

DDist is the number of trees in DCLASS diameter class and TPDfifteen is the initial number of trees in the 15 cm diameter class (Figure 12).

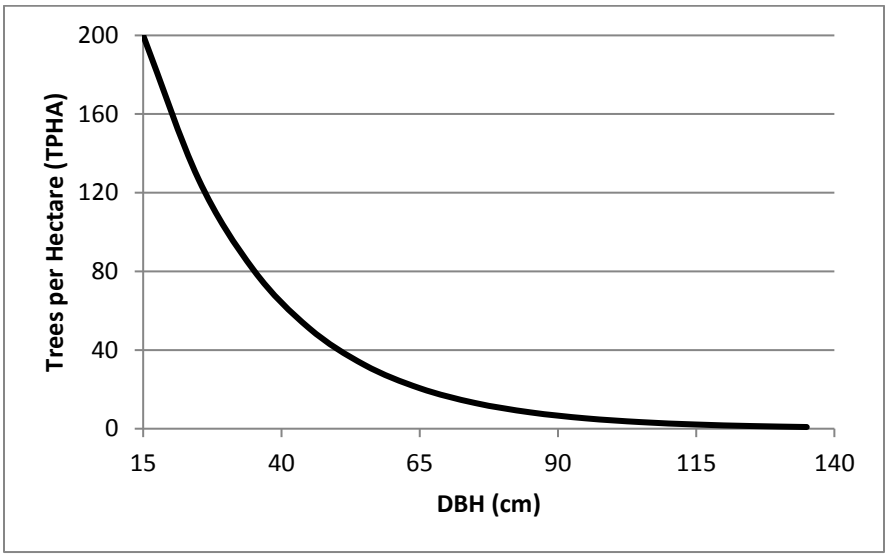

Figure 12: Inverse-J function used to determine diameter distribution.

The initial distribution is further modified multiple times. After determining and rounding the number of trees in each diameter class, the trees are distributed along the two categories of position (edge vs. interior), the two categories of damage, and the three levels of crown infection for red fir. The distribution used is equivalent to the distribution of the categories found in the collected data. The values are rounded to whole numbers and the fields for the first year (year 0) are automatically populated.

Treatment must be executed manually. The treatment page has cells to enter that indicate how many trees from each size class are to be removed. A treatment was executed after 21 years of growth. One third of the trees in each cell between 15 cm and 75 cm size classes were removed in order to simulate a thin from below. Trees over 75 cm were excluded from treatment

due to the California size restriction. Mortality and ingrowth also influence the distribution of trees.

Ingrowth and Mortality

Not much information exists for predicting ingrowth or mortality relative to SDI. Studies indirectly related to SDI exist for mixed conifer forests in the Sierra Nevada (Mutch & Parsons 1998, van Mantgem et al. 2003, van Mantgem & Stephenson, 2005) and a study for all of California with respect to red fir mortality in particular (Mortensen 2011). Since these studies do not report formulas that would apply to this study, it was decided against attempting to reconstruct ingrowth from these studies. Instead, an intuitive formula was chosen that uses the chi-squared distribution with six degrees of freedom ($k = 6$) to produce a skewed bell shaped curve. This function was used since it has a value of zero ingrowth trees for a SDI of zero, has an apex that can be determined by the user in terms of the amplitude, the position of the apex can be modified along differing values of SDI, and has a value close to zero trees for maximum stand densities. The ingrowth function is

$$IG = (c \times TRTTIME \times a \times IGMAX) \times \left(\left(\left(\frac{SDI}{b \times SDIINFL}\right)^2\right) \times e^{\frac{-\frac{SDI}{b*SDIINFL}}{2}}\right)/16$$

where IG is the number of trees that have a diameter of 10 cm, a = 7.3888, b = 0.25, c = 0.05, e is the natural log, TRTTIME is the time since the last treatment, IGMAX is the maximum number of trees, and SDIINFL is the value in SDI units that the user believes would produce the most trees (Figure 13). IGMAX and SDIINFL are entered on the initial conditions worksheet.

Considering the damaging effects that logging has on smaller trees, and not wanting mortality to account for this, it was decided that a treatment would likely substantially damage

ingrowth and that it would take about 20 years for normal ingrowth rates to resume. Therefore, if treatment time was less than 20 years, a proportion of the expected ingrowth without a recent treatment would occur, e.g., if 10 years occurred since the last treatment, half of what would be expected to grow at 20 years would occur. Every fifth year, starting at year five, this function is implemented using the values from the previous year since ingrowth for the current year should be represented by the population from the previous year. The values were then rounded and distributed according to the initial position/damage/crown infection ratios.

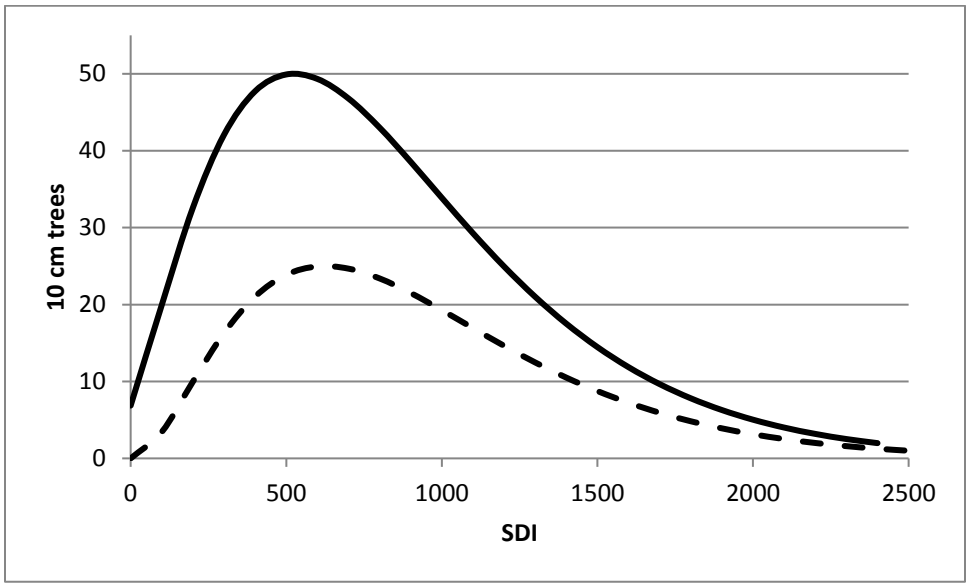

Figure 13: Represents 5 years worth of ingrowth. The solid line represents the amount of ingrowth in the 10 cm size class after 5 years of growth and after 20 years or more since the previous treatment. The dashed line represents ingrowth after 10 years since the previous treatment.

Equations for mortality with regard to SDI were similarly difficult. Van Mantgem et al. (2003) produced a formula for white fir mortality based on diameter increment; the lower diameter increment, the more likely the tree would die. Mortensen (2011) also created a model for mortality for red fir which included variables such as damage, quadratic mean diameter, and

stand age. Mutch and Parson (1998) also looked at mortality and reported results that varied unpredictably. This simulator uses a modified version of the inverse J-shaped curve that was created for the initial diameter distribution. This curve is J-shaped and has a value of 1 at 2500 SDI units (Figure 14). The equation is

$$Mort = DLTASDI \times e^{\frac{SDI-2500}{21.795*ATSIXTY+190.21}}$$

where DLTASDI is the amount SDI has increased over the past five years, ATSIXTY is the percent of mortality of DLTASDI the user wants to occur in terms of SDI units at 60% of the maximum SDI, which is 2500 for these stands. The value 20 was chosen to indicate a mortality of 20% of the change in SDI to occur when the stand has a value of 60% of the maximum SDI, or 1500 for these stands. The ATSIXTY value is significant because it is considered the value at which mortality is imminent according to Reineke (1938). The original distribution was again used to distribute the mortality after turning SDI values into trees per size class and implemented every five years starting at year 6 due to the execution of ingrowth in five year increments starting at year 5.

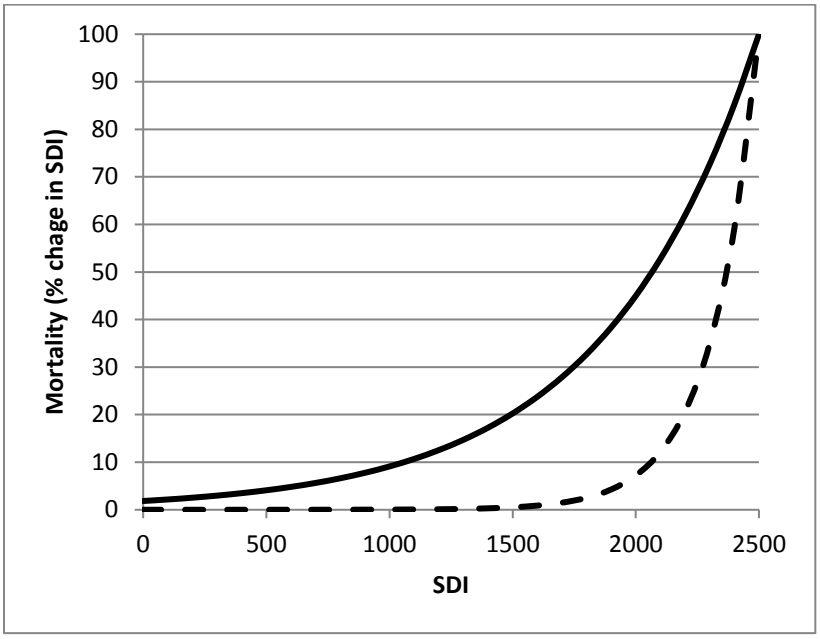

Figure 14: Mortality as a percent change in SDI from the previous 5 years of growth. The solid line illustrates an ATSIXTY value of 20, resulting in 20.2% mortality 60% max SDI. This was used for the simulations in this study. The dashed line illustrates an ATSIXTY value of 0, resulting in 0.5% mortality at 60% max SDI.

A series of worksheets was created to determine one year's worth of growth and the corresponding SDI and WF.SDI. The first worksheet establishes the initial conditions including SITE, LAT.ADJ.ELEV, TRMI.NO.DR, and the parameters for ingrowth and mortality. In addition, worksheets were created for: the treatment, DBH of each tree in each cell, SDI for each tree in each cell, total SDI of each cell (number of trees times the SDI for each tree) and for the stand, SDIL for each cell, BA for each tree in each cell, mortality for each cell, HT:DBH for each tree in each cell based on the function, height for each tree based on the HT:DBH equation, HT:DBH for each tree in each cell after ensuring the trees did not shrink since the previous year, CR for each tree in each cell based on the function, base of the live crown (BLC) for each tree in each cell from the CR function, CR for each tree in each cell after ensuring the live crown did

not recede, BAI for each tree in each cell based on the function, BA after adding BAI for each tree in each cell, and diameter increment (DI) for each tree in each cell. DI is then added to the DBH of each tree in each cell so that the cells for the following year are populated with the sizes differing for each cell since each cell will have experienced different amounts of growth. WF.SDI is computed annually from the distribution within the SDI worksheet. Ingrowth occurs within the original distribution worksheet. Table 12 and Table 13 illustrate how the terms and the worksheets relate so that each year's total stand growth can be determined, and to show how SDI and WF.SDI change over time.

Table 12: Simulator original inputs determined by user.

Original inputs
1. Site (Klamath, Sequoia, or Tahoe)
2. Aspect (°)
3. Slope (°)
4. Horizontal Configuration (0 to 10 for convex to concave)
5. Topographic position (% from top to bottom)
6. Elevation
7. SDI inflection point for ingrowth
8. Maximum ingrowth
9. Mortality of 5 yr accumulated SDI > 1500 (%)
10. Number of trees in 15 cm DBH class
11. WF.SDI (%)
12. Treatment
13. Proportion of trees on edges (%)
14. Proportion of trees with damage (%)
15. Proportion of trees with levels of cytospora infection (%)

Table 13: Illustrates the relationships between terms so that BAI, SDI, and treatment persistence can be determined from inputs. The new year's DBH is determined by the previous year's DBH and the calculated diameter increment (DI). This is where the simulator loops in order to calculate annual growth.

Outputs	Related inputs
A. TRMI.NO.DR	2, 3, 4, 5
B. LAT.ADJ.ELEV (m)	1, 6
C. Ingrowth (5 year increments)	7, 8, I
D. Mortality (5 year increments)	9, I
E. DBH Distribution	10, 11, 12, 13, 14, 15, C, D
F. Individual tree DBH (cm)	E, U[a]
G. Individual tree SDI	F
H. SDI distribution	E, G
I. SDI total	H
J. WF.SDI (%)	11, H, I
K. SDIL	H
L. BA_0 (cm^2)	G
M. $HT:DBH_0$ (m/cm)	1, 13, A (red fir), B, G, I (white fir), K (red fir)
N. HT (m)	F, M
O. $HT:DBH_1$ (m/cm)	F, M, N
P. CR_0	1, 13, F, I, O
Q. BLC (m)	N, P
R. CR_1	N, Q
S. BAI (cm^2)	1, 13 (white fir), 14, 15 (red fir), A, F, J (white fir), K, R
T. BA_1 (cm^2)	F, S
U. DI (cm)	F, T[b]

a: This is where the simulator loops.
b: The end of the simulator loop.

Twelve scenarios were created in order to illustrate how different conditions and compositions influence stand growth. The three different sites were represented, two different initial compositions, and two different moisture levels. The three sites are represented by S, K, and T for Sequoia, Klamath, and Tahoe. The two different moisture levels are represented by M and D for 75% max TRMI.NO.DR (45 TRMI units) for moist and 25% max TRMI.NO.DR (15 TRMI units) for dry respectively. The greatest common latitude adjusted elevation (LAT.ADJ.ELEV) was used for the red fir dominated stands while the least common LAT.ADJ.ELEV was used for the white fir dominated stands. Red fir dominated stands and white fir dominated stands are represented by R and W respectively. The original distribution for the red fir dominated stands included 75% red fir in the smallest diameter class and then the rest of the cells were populated as mentioned above. Similarly, the original distribution for white fir dominated stands included the same 75% white fir in the smallest diameter class. The different scenarios are represented by a three letter code. For example, a stand in Sequoia, dominated by red fir, and on a moist site is represented as SRM.

Results

Initial populations are represented below. Initial populations for stands that are composed of 75% white fir SDI are illustrated in Table 14, Table 16, and Table 17. Initial populations for stands composed of 25% white fir SDI are illustrated in Table 15, Table 18, and Table 19. Population distribution based on DBH is the results of the DDist

function are the sum of the categorical distribution (not illustrated). Distribution proportions based on those recorded in the sampling are illustrated in the category labels.

Table 14: Initial white fir distribution for 75% white fir in 15 cm size class. See Table 16 and Table 17 for accompanying distributions.

DBH	Interior, mild damage 53%[a]	Interior, major damage 9%	Edge, mild damage 30%	Edge, major damage 8%
15	80	14	45	12
25	50	9	29	8
35	32	5	18	5
45	20	3	11	3
55	13	2	7	2
65	8	1	5	1
75	5	1	3	1
85	3	1	2	0
95	2	0	1	0
105	2	0	1	0
115	1	0	1	0
125	1	0	0	0
135	1	0	0	0

a: Distribution of trees sampled

Table 15: Initial white fir distribution for 25% white fir in 15 cm size class. See Table 18 and Table 19 for accompanying distributions.

DBH	Interior, mild damage	Interior, major damage	Edge, mild damage	Edge, major damage
15	27	5	15	4
25	17	3	10	3
35	11	2	6	2
45	7	1	4	1
55	4	1	2	1
65	3	0	2	0
75	2	0	1	0
85	1	0	1	0
95	1	0	0	0
105	1	0	0	0
115	1	0	0	0
125	0	0	0	0
135	0	0	0	0

Table 16: Initial red fir interior distribution for 75% white fir in 15 cm size class. See Table 14 Table 17 for accompanying distributions.

DBH	Mild damage, CI 0 37%[a]	Mild damage, CI 1 12%	Mild damage, CI 2 4%	Major damage, CI 0 6%	Major damage, CI 1 2%	Major damage, CI 2 1%
15	19	6	2	3	1	1
25	12	4	1	2	1	0
35	7	2	1	1	0	0
45	5	2	1	1	0	0
55	3	1	0	0	0	0
65	2	1	0	0	0	0
75	1	0	0	0	0	0
85	1	0	0	0	0	0
95	0	0	0	0	0	0
105	0	0	0	0	0	0
115	0	0	0	0	0	0
125	0	0	0	0	0	0
135	0	0	0	0	0	0

a: Distribution of trees sampled.

Table 17: Initial red fir edge distributions for 75% white fir in 15 cm size class. See Table 14 and Table 16 for accompanying distributions.

DBH	Mild damage, CI 0 22%	Mild damage, CI 1 6%	Mild damage, CI 2 2%	Major damage, CI 0 5%	Major damage, CI 1 2%	Major damage, CI 2 1%
15	11	3	1	3	1	1
25	7	2	1	2	1	0
35	4	1	0	1	0	0
45	3	1	0	1	0	0
55	2	0	0	0	0	0
65	1	0	0	0	0	0
75	1	0	0	0	0	0
85	0	0	0	0	0	0
95	0	0	0	0	0	0
105	0	0	0	0	0	0
115	0	0	0	0	0	0
125	0	0	0	0	0	0
135	0	0	0	0	0	0

Table 18: Initial red fir interior distribution for 25% white fir in 15 cm size class. See Table 15 and Table 19 for accompanying distributions.

DBH	Mild damage, CI 0	Mild damage, CI 1	Mild damage, CI 2	Major damage, CI 0	Major damage, CI 1	Major damage, CI 2
15	56	18	6	9	3	2
25	36	12	4	6	2	1
35	23	7	2	4	1	1
45	14	5	2	2	1	0
55	9	3	1	1	0	0
65	6	2	1	1	0	0
75	4	1	0	1	0	0
85	2	1	0	0	0	0
95	1	0	0	0	0	0
105	1	0	0	0	0	0
115	1	0	0	0	0	0
125	0	0	0	0	0	0
135	0	0	0	0	0	0

Table 19: Initial red fir exterior distribution for 25% white fir in 15 cm size class. See Table 15 and Table 18 for accompanying distributions.

DBH	Mild damage, CI 0	Mild damage, CI 1	Mild damage, CI 2	Major damage, CI 0	Major damage, CI 1	Major damage, CI 2
15	33	9	3	8	3	2
25	21	6	2	5	2	1
35	13	4	1	3	1	1
45	9	2	1	2	1	0
55	5	1	0	1	0	0
65	4	1	0	1	0	0
75	2	1	0	1	0	0
85	1	0	0	0	0	0
95	1	0	0	0	0	0
105	1	0	0	0	0	0
115	0	0	0	0	0	0
125	0	0	0	0	0	0
135	0	0	0	0	0	0

There are more similarities than differences when comparing the models. Statistics for terms not used in Chapter 1 are represented in Table 20 through Table 23. The logit transformation was used on CR because the values range between 0 and 1. The natural log (log) transformation was used on the HT:DBH because it resulted in better adjusted R-squared values and residual tests indicated better fit than other no transformation or cube root transformations. Log transformations were also used on SDI and DBH predictor variables for the best CR model for red fir. The differences for HT:DBH models include the term SDIL for the best white fir HT.DBH as opposed to SDI for the red fir model and the inclusion of the term TRMI.NO.DR for the red fir model where it is not included in the white fir model.

Table 20: Statistics for terms used for modeling red fir CR and HT:DBH not represented in Chapter 1.

Term	Min	Median	Mean	Max
SDI	125.4	843	932.2	2516
HT (m)	4.3	18.4	20.51	51.2
HT.DBH (m/cm)	0.2129	0.5054	0.5049	1.041

Table 21: Statistics for terms used for modeling white fir CR and HT:DBH not represented in Chapter 1.

Term	Min	Median	Mean	Max
SDI	112.1	825.1	964.3	2370
HT (m)	5.4	17.4	20.67	59.2
HT.DBH (m/cm)	0.2999	0.4873	0.5109	0.8632

Table 22: Elevation (m) statistics for red fir.

SITE	Min	Mean	Median	Max	Count
TNF	1939.82	2168.17	2167.19	2402.93	53
SNF	2065.80	2271.87	2255.93	2499.94	37
KNF	1496.77	1693.40	1688.08	1873.14	47

Table 23: Elevation (m) statistics for white fir.

SITE	Min	Mean	Median	Max	Count
TNF	1915.56	2031.55	2030.99	2155.25	39
SNF	2073.25	2261.62	2230.1	2456.11	39
KNF	1354.08	1690.16	1715.39	1873.14	53

When comparing adjusted R-squared results, it is evident that the CR and HT:DBH models were substantially less predictive than for the BAI driver models. The values were better for the HT:DBH models at 0.55 and 0.60, for red fir and white fir respectively, than for the CR models, 0.46 and 0.37. The ultimate influence of these errors on treatment persistence, final SDI, and WF.SDI values was not determined since the simulator does not include an option for varying error terms. Included are summaries for best red fir and white fir CR and HT:DBH models, bootstrapping results for each model's coefficients in terms of bias and standard errors (Table 24 through Table 31).

Table 24: R summary of best model coefficients for red fir crown ratio (CR). The best model is represented by the formula: logit(CR) ~ log(SDI) + log(DBH) + HT.DBH + EDGE.YN + SITE. (Residual standard error: 0.5995 on 130 degrees of freedom, Multiple R-squared: 0.4843, Adjusted R-squared: 0.4605, F-statistic: 20.35 on 6 and 130 DF, p-value: < 2.2e-16)

Coefficients	Estimate	Std. Error	t value	Pr(>|t|)	
(Intercept)	5.654	0.74657	7.573	5.98E-12	***[a]
log(SDI)	-0.4713	0.09738	-4.84	3.62E-06	***
log(DBH)	-0.39401	0.08549	-4.609	9.55E-06	***
HT.DBH	-0.97696	0.57659	-1.694	0.09259	.
EDGE.YN	0.54039	0.11624	4.649	8.08E-06	***
SITESNF	0.43208	0.15398	2.806	0.00579	**
SITETNF	0.14468	0.14118	1.025	0.30734	

a: Significance codes: 0 '***' 0.001 '**' 0.01 '*' 0.05 '.' 0.1 ' ' 1

Table 25: Ordinary nonparametric bootstrap statistics with 10,000 replications for red fir CR model coefficients.

Coefficients	Original	Bias	Standard error	Adjusted confidence interval
(Intercept)	5.6540048	0.03274719	0.71558134	(4.205, 7.032)
log(SDI)	-0.4713002	-0.00138788	0.08394895	(-0.6423, -0.3101)
log(DBH)	-0.3940143	-0.00401286	0.0824661	(-0.5545, -0.2327)
HT.DBH	-0.9769648	-0.01380862	0.59814739	(-2.1156, 0.2326)
EDGE.YN	0.5403874	-0.00414206	0.12189976	(0.3023, 0.7773)
SITESNF	0.4320842	-0.00047597	0.16006581	(0.1238, 0.7437)
SITETNF	0.1446822	-0.00388039	0.13631808	(-0.1248, 0.4103)

Table 26: R summary of best model coefficients for white fir crown ratio (CR). The best model is represented by the formula: logit(CR) ~ SDI + DBH + HT .DBH + EDGE.YN + SITE. (Residual standard error: 0.6304 on 124 degrees of freedom, Multiple R-squared: 0.3965, Adjusted R-squared: 0.3673, F-statistic: 13.58 on 6 and 124 DF, p-value: 8.386e-12)

Coefficients	Estimate	Std. Error	t value	Pr(>|t|)	
(Intercept)	2.1290767	0.4568978	4.66	8.03E-06	***[a]
SDI	-0.0005099	0.0001358	-3.754	0.000266	***
DBH	-0.0061785	0.0021097	-2.929	0.004053	**
HT.DBH	-1.4719178	0.7297783	-2.017	0.045862	*
EDGE.YN	0.4267296	0.1376861	3.099	0.002401	**
SITESNF	0.2930591	0.1506003	1.946	0.053924	.
SITETNF	0.416877	0.1500475	2.778	0.006315	**

a: Significance codes: 0 '***' 0.001 '**' 0.01 '*' 0.05 '.' 0.1 ' ' 1

Table 27: Ordinary nonparametric bootstrap statistics with 10,000 replications for white fir CR model coefficients.

Coefficients	Original	Bias	Standard error	Adjusted confidence interval
(Intercept)	2.129076662	8.63E-03	0.481355538	(1.19827, 3.085679)
SDI	-0.000509855	-1.51E-06	0.000125301	(-7.4734e-4, -2.5576e-4)
DBH	-0.000617845	1.48E-05	0.002043739	(-0.01022, -0.00214)
ht.DBH	-1.471917817	-1.07E-02	0.717905937	(-2.866419, -0.02618409)
EDGE.YN	0.426729612	3.20E-04	0.141904717	(0.1562566, 0.7090127)
SITESNF	0.293059077	-7.13E-03	0.162550828	(-0.02051452, 0.6158981)
SITETNF	0.416877031	-3.33E-03	0.149223213	(0.1292845, 0.7160214)

Table 28: R summary of the best model coefficients for red fir height to diameter ratio (HT:DBH). The best model is represented by the formula: log(HT.DBH) ~ DBH + SDI + SITE + LAT.ADJ.ELEV + TRMI.NO.DR + EDGE.YN. (Residual standard error: 0.1608 on 129 degrees of freedom, Multiple R-squared: 0.5756, Adjusted R-squared: 0.5526, F-statistic: 25 on 7 and 129 DF, p-value: < 2.2e-16)

Coefficients	Estimate	Std. Error	t value	Pr(>|t|)	
(Intercept)	0.0076067	2.69E-01	0.028	0.9775	[a]
DBH	-0.0034174	5.04E-04	-6.775	3.98E-10	***
SDI	0.0001384	2.99E-05	4.628	8.88E-06	***
SITESNF	-0.2829723	4.68E-02	-6.046	1.49E-08	***
SITETNF	-0.1930943	4.10E-02	-4.709	6.33E-06	***
LAT.ADJ.ELEV	-0.0003563	1.40E-04	-2.544	0.0121	*
TRMI.NO.DR	0.0023477	1.70E-03	1.38	0.1698	
EDGE.YN	-0.0789036	3.16E-02	-2.496	0.0138	*

a: Significance codes: 0 '***' 0.001 '**' 0.01 '*' 0.05 '.' 0.1 ' ' 1

Table 29: Ordinary nonparametric bootstrap statistics with 10,000 replications for red fir HT:DBH model coefficients.

Coefficients	Original	Bias	Standard error	Adjusted confidence interval
(Intercept)	0.00760668	7.16E-03	2.99E-01	(-0.5217, 0.6756)
DBH	-0.00034174	1.43E-06	4.68E-05	(-4.3410e-4, -2.5255e-4)
SDI	0.00013839	-6.80E-07	3.14E-05	(7.4622e-05, 1.9912e-4)
SITESNF	-0.28297234	-1.27E-03	4.75E-02	(-0.3821, -0.1946)
SITETNF	-0.19309426	4.50E-04	4.67E-02	(-0.2791, -0.0939)
LAT.ADJ.ELEV	-0.00035628	-3.70E-06	1.54E-04	(-7.0014e-4, -8.2482e-05)
TRMI.NO.DR	0.00234773	-1.55E-05	1.72E-03	(-1.1359e-3, 5.6823e-3)
EDGE.YN	-0.07890359	-5.79E-04	2.90E-02	(-0.1361, -0.0215)

Table 30: R summary of best model coefficients for white fir height to diameter ratio (HT:DBH). The best model is represented by the formula: log(HT.DBH) ~ DBH + SDIL + LAT.ADJ.ELEV + SITE + EDGE.YN. (Residual standard error: 0.1315 on 124 degrees of freedom, Multiple R-squared: 0.6141, Adjusted R-squared: 0.5955, F-statistic: 32.89 on 6 and 124 DF, p-value: < 2.2e-16)

Coefficients	Estimate	Std. Error	t value	Pr(>|t|)	
(Intercept)	2.69E-01	2.03E-01	1.327	0.18688	[a]
DBH	-2.48E-03	4.44E-04	-5.584	1.41E-07	***
SDIL	1.52E-04	3.21E-05	4.739	5.79E-06	***
LAT.ADJ.ELEV	-4.96E-04	1.18E-04	-4.212	4.83E-05	***
SITESNF	-2.43E-01	3.80E-02	-6.39	3.04E-09	***
SITETNF	-1.69E-01	2.80E-02	-6.052	1.57E-08	***
EDGE.YN	-7.74E-02	2.74E-02	-2.827	0.00548	**

a: Significance codes: 0 '***' 0.001 '**' 0.01 '*' 0.05 '.' 0.1 ' ' 1

Table 31: Ordinary nonparametric bootstrap statistics with 10,000 replications for white fir HT:DBH model coefficients.

Coefficients	Original	Bias	Standard error	Adjusted confidence interval
(Intercept)	0.26936936	-9.79E-04	1.91E-01	(-0.0961, 0.6603)
DBH	-0.00248085	1.06E-05	4.04E-04	(-3.2984e-03, -1.7073e-02)
SDIL	0.00015185	-1.58E-07	3.87E-05	(7.0465e-05, 2.242794e-04)
LAT.ADJ.ELEV	-0.00049579	7.14E-07	1.12E-04	(-7.2228e-04, -2.7677e-04)
SITESNF	-0.24309362	-1.20E-04	3.64E-02	(-0.3121, -0.1679)
SITETNF	-0.16935511	-7.15E-05	2.89E-02	(-0.2252, -0.1118)
EDGE.YN	-0.07737454	-6.72E-04	2.51E-02	(-0.1253, -0.0275)

Distributions after 22 years of growth differed slightly between scenarios. TWM and TRM are two of the average distributions after 22 years (Table 32 through Table 37).

The sections below DBH_0 indicate which year the trees grew in to the stand. Scenarios that had less density experienced more ingrowth and scenarios with more density experienced more mortality. The difference in ingrowth and mortality between TWM and the best and worst performing white fir dominated scenarios, as well as the difference between TRM and the best and worst performing red fir dominated scenarios are illustrated in Table 30.

Table 32: TWM year 22 white fir distribution for 75% white fir in 15 cm initial size class. This is the distribution after 22 years of growth, mortality, ingrowth, and one third of the 15 cm to 65 cm size classes thinned. Refer to Table 34 and Table 35 for accompanying distributions.

	DBH_0	Interior, mild damage	Interior, major damage	Edge, mild damage	Edge, major damage
yr 20	10	11	2	6	2
yr 15	10	13	2	7	2
yr 10	10	15	3	8	2
yr 5	10	17	3	10	3
	15	46	9	27	8
	25	31	6	19	5
	35	21	3	12	3
	45	14	3	8	2
	55	9	1	5	1
	65	5	1	3	1
	75	3	1	2	1
	85	2	1	1	0
	95	1	0	1	0
	105	1	0	1	0
	115	1	0	1	0
	125	1	0	0	0
	135	1	0	0	0

Table 33:TRM year 22 white fir distribution for 25% white fir in 15 cm initial size class. This is the distribution after 22 years of growth, mortality, ingrowth, and one third of the 15 cm to 65 cm size classes thinned. Refer to Table 36 and Table 37 for accompanying distributions.

	DBH_0	Interior, mild damage	Interior, major damage	Edge, mild damage	Edge, major damage
yr 20	10	4	1	2	1
yr 15	10	5	1	3	1
yr 10	10	5	1	3	1
yr 5	10	6	1	3	1
	15	15	3	10	3
	25	11	2	7	2
	35	7	1	4	1
	45	5	1	3	1
	55	3	1	1	1
	65	2	0	1	0
	75	1	0	1	0
	85	1	0	1	0
	95	1	0	0	0
	105	1	0	0	0
	115	1	0	0	0
	125	0	0	0	0
	135	0	0	0	0

Table 34: TWM year 22 red fir interior distribution for 75% white fir in 15 cm initial size class. This is the distribution after 22 years of growth, mortality, ingrowth, and one third of the 15 cm to 65 cm size classes thinned. Refer to Table 32 and Table 35 for accompanying distributions.

	DBH_0	Mild damage, CI 0	Mild damage, CI 1	Mild damage, CI 2	Major damage, CI 0	Major damage, CI 1	Major damage, CI 2
yr 20	10	2	1	0	0	1	0
yr 15	10	2	1	0	0	1	0
yr 10	10	3	1	0	0	1	0
yr 5	10	3	1	0	0	1	0
	15	10	4	1	2	1	1
	25	8	3	1	1	1	0
	35	5	1	1	1	0	0
	45	3	1	1	1	0	0
	55	2	1	0	0	0	0
	65	1	1	0	0	0	0
	75	1	0	0	0	0	0
	85	1	0	0	0	0	0
	95	0	0	0	0	0	0
	105	0	0	0	0	0	0
	115	0	0	0	0	0	0
	125	0	0	0	0	0	0
	135	0	0	0	0	0	0

Table 35: TWM year 22 red fir exterior distribution for 75% white fir in 15 cm initial size class. This is the distribution after 22 years of growth, mortality, ingrowth, and one third of the 15 cm to 65 cm size classes thinned. Refer to Table 32 and Table 34 for accompanying distributions.

	DBH_0	Mild damage, CI 0	Mild damage, CI 1	Mild damage, CI 2	Major damage, CI 0	Major damage, CI 1	Major damage, CI 2
yr 20	10	1	0	0	0	0	0
yr 15	10	1	0	0	0	0	0
yr 10	10	2	0	0	0	0	0
yr 5	10	2	0	0	0	0	0
	15	7	2	1	2	1	1
	25	5	1	1	1	1	0
	35	3	1	0	1	0	0
	45	2	1	0	1	0	0
	55	1	0	0	0	0	0
	65	1	0	0	0	0	0
	75	1	0	0	0	0	0
	85	0	0	0	0	0	0
	95	0	0	0	0	0	0
	105	0	0	0	0	0	0
	115	0	0	0	0	0	0
	125	0	0	0	0	0	0
	135	0	0	0	0	0	0

Table 36: TRM year 22 red fir interior distribution for 25% white fir in 15 cm initial size class. This is the distribution after 22 years of growth, mortality, ingrowth, and one third of the 15 cm to 65 cm size classes thinned. Refer to Table 33 and Table 37 for accompanying distributions.

	DBH_0	Mild damage, CI 0	Mild damage, CI 1	Mild damage, CI 2	Major damage, CI 0	Major damage, CI 1	Major damage, CI 2
yr 20	10	7	2	1	1	1	0
yr 15	10	8	3	1	1	1	0
yr 10	10	10	3	1	2	1	0
yr 5	10	11	3	1	2	1	0
	15	32	9	4	6	2	1
	25	21	8	3	4	1	1
	35	15	5	1	3	1	1
	45	9	3	1	1	1	0
	55	6	2	1	1	0	0
	65	4	1	1	1	0	0
	75	3	1	0	1	0	0
	85	1	1	0	0	0	0
	95	1	0	0	0	0	0
	105	1	0	0	0	0	0
	115	1	0	0	0	0	0
	125	0	0	0	0	0	0
	135	0	0	0	0	0	0

Table 37: TRM year 22 red fir exterior distribution for 25% white fir in 15 cm initial size class. This is the distribution after 22 years of growth, mortality, ingrowth, and one third of the 15 cm to 65 cm size classes thinned. Refer to Table 33 and Table 36 for accompanying distributions.

	DBH_0	Mild damage, CI 0	Mild damage, CI 1	Mild damage, CI 2	Major damage, CI 0	Major damage, CI 1	Major damage, CI 2
yr 20	10	4	1	0	1	0	0
yr 15	10	5	1	0	1	0	0
yr 10	10	6	2	1	1	1	0
yr 5	10	6	2	1	1	1	0
	15	19	6	2	5	2	1
	25	14	4	1	3	1	1
	35	9	3	1	2	1	1
	45	6	1	1	1	1	0
	55	3	1	0	1	0	0
	65	3	1	0	1	0	0
	75	1	1	0	1	0	0
	85	1	0	0	0	0	0
	95	1	0	0	0	0	0
	105	1	0	0	0	0	0
	115	0	0	0	0	0	0
	125	0	0	0	0	0	0
	135	0	0	0	0	0	0

Table 38: Illustrates the difference between the scenarios with the best performance and worst performance compared to scenarios with average performance.

Scenario	White fir ingrowth	White fir mortality	Red fir ingrowth	Red fir mortality
TRM	39	47	96	144
SRM	-6	+3	-12	+4
TWM	106	147	24	40
KWD	+10	-5	+4	-3

Unfortunately, rounding errors influence how the tree distributions are executed. This is true for the initial distribution, ingrowth, mortality, and the treatment if the treatment was determined by dividing the population as was done in this study. The issue is due to values distributed over a large numbers of cells and the need for whole numbers of trees. When rounding, those small decimals often default to zero. Larger trees and trees with conditions that are populated less frequently, such as red fir trees with high degrees of cytospora infection and major damage which make up only 2% of the population are rarely populated and, if so, rarely influenced by mortality. Ingrowth also experiences a general reduction in population as well. A repeatable and reasonable solution has not been determined.

Table 39 illustrated the results of the 12 scenarios run in the simulator. Although it was originally established that the first size class in the W stands would have 75% white fir, it did not result in 75% WF.SDI because the workbook distributed the values and rounded the numbers. This is because there is the additional term, CRN.INFECT

included in the red fir models. This skewed the distribution and resulted in an initial WF.SDI of 0.80 for white fir dominated stands and 0.27 for red fir dominated stands.

Scenarios ranked predictably when considering results from Chapter 2. Treatment persistence and final SDI are grouped for comparison purposes in Table 40. In terms of treatment persistence, the top three scenarios were Sequoia sites. Five of the top seven scenarios were moist. Four of the top five scenarios were red fir dominated. The two lowest scenarios represent Klamath, Tahoe, white fir, and dry. This illustrates that Sequoia was generally a better growing site, red fir dominated stands were generally more productive than white fir dominated stands, and moist stands are more productive than drier stands.

Table 39: Different scenarios run and corresponding WF.SDI and SDI values. The scenario names correspond to S for Sequoia, K for Klamath, T for Tahoe, W for 75% white fir of initial 15 cm diameter distribution, R for 25% white fir of initial 15 cm diameter distribution, M for 75% max TRMI.NO.DR, and D for 25% max TRMI.NO.DR.

	Time (years)	WF.SDI	SDI		Time (years)	WF.SDI	SDI		Time (years)	WF.SDI	SDI
SWM:	0	0.80	900	KWM:	0	0.80	900	TWM:	0	0.80	900
	21	0.77	1380		21	0.78	1225		21	0.80	1299
	22	0.76	987		22	0.76	873		22	0.79	924
	42	0.74	1386		48	0.74	1226		45	0.79	1308
	50	0.73	1554		50	0.74	1261		50	0.79	1394
SWD:	0	0.80	900	KWD:	0	0.80	900	TWD:	0	0.80	900
	21	0.78	1278		21	0.79	1146		21	0.80	1203
	22	0.77	910		22	0.77	815		22	0.79	855
	45	0.75	1279		55	0.75	1149		50	0.80	1211
	50	0.75	1362		50	0.75	1102		50	0.80	1211
SRM:	0	0.27	890	KRM:	0	0.27	890	TRM:	0	0.27	890
	21	0.27	1463		21	0.27	1285		21	0.30	1292

	Time (years)	WF.SDI	SDI
	22	0.27	1079
	39	0.27	1472
	50	0.27	1721
SRD:	0	0.27	890
	21	0.27	1333
	22	0.27	983
	41	0.27	1333
	50	0.27	1509

	Time (years)	WF.SDI	SDI
	22	0.27	948
	43	0.27	1291
	50	0.27	1417
KRD:	0	0.27	890
	21	0.27	1189
	22	0.27	878
	48	0.27	1197
	50	0.27	1229

	Time (years)	WF.SDI	SDI
	22	0.30	953
	43	0.32	1303
	50	0.33	1432
TRD:	0	0.27	890
	21	0.29	1196
	22	0.30	883
	47	0.32	1198
	50	0.33	1243

Table 40: Treatment persistence for each scenario compared to rank of SDI at year 50. Asterisk denotes ranking switched compared to treatment persistence

Scenario	TP (years)	Scenario	SDI at year 50
SRM	17	SRM	1721
SRD	19	SWM*	1554
SWM	20	SRD*	1509
TRM	21	TRM	1432
KRM	21	KRM	1417
TWM	23	TWM	1394
SWD	23	SWD	1362
TRD	25	KWM*	1261
KWM	26	TRD*	1243
KRD	26	KRD	1229
TWD	28	TWD	1211
KWD	33	KWD	1102

Discussion

CR and HT:DBH models

SDI and SDIL are present in all of the models created in this study. Crown ratio models give further insight into how stand density and edge effects influence individual tree growth. Although SDIL is a superior term in both BAI models, SDI is superior in both CR models. This indicates that both density of trees larger than the target tree and total neighboring density influence BAI, the former more directly and the latter more indirectly. SDI may be a better predictor for these CR models due to the fact that CR was

not measured from the average of lowest live branches but rather the lowest live branch itself. In this case, the lowest live branch has a better correlation with all of the competition rather than the competition attributed to trees larger than the target tree since light will be available lower in the tree if it is maintaining live leaf area due to irregular canopy spacing.

It is also of interest that the best red fir HT:DBH model contains the term SDI while the best white fir model includes the term SDIL. It is unclear as to why either total density or the density attributable to trees larger than the target tree would have a different influence. The term that is only present in one of the four models created for this chapter is the TRMI.NO.DR term included in the red fir HT.DBH model. It makes sense that it would be present due to the hydrological limitations of tree height (Koch et al. 2004). As to why it is not present in the white fir model is unclear. One reason may be that moisture availability varies greatly over a tree's lifetime and it may be too inconsistent to be a strong predictor.

The interaction between height to diameter ratio and crown ratio is both intuitive and counterintuitive. It was hypothesized in Chapter 2 that elevation and its interactions would be variables found in the best BAI models. This was not the case. The only time that elevation showed up was for HT:DBH models. This might be because adjusting for elevation over such a wide range of latitude leaves substantial room for error. The overlap of elevation between the range of the highest and range of the lowest sites in terms of latitude adjusted elevation is only about 140 m, whereas the average change of

elevation for all of the sites is around 490 m. If this study were repeated, it would be better to disregard the latitude adjusted elevation formula and instead rely on the data itself to illustrate where the transition from red fir to white fir actually is. This might give more useful results.

Elevation becomes influential because LAT.ADJ.ELEV, HT:DBH, and CR are all related. As elevation increases, HT:DBH decreases. As HT:DBH decreases, CR increases and vice versa. It makes sense that trees get shorter as elevation increases due to the harsher climate and the more spaced out trees (personal observation). It also makes sense that trees that have lower HT:DBH values likely have longer crowns since they are more likely open grown. The interesting interaction occurs for trees at higher elevations. The combination indicates that trees at higher elevations grow more than trees at lower elevations for both species because trees with greater CR grow more vigorously. This might be part of the reason that elevation is not a better predictor. Almost all growth models have crown ratio as one of the predictor variables and trees at higher elevations have longer crowns if the environment is harsher which counteracts the notion that trees at higher elevations grow more poorly. More research is needed to better understand this.

Simulator performance

The simulator performed as the BAI models from Chapter 2 suggested it would. Although red fir trees do not generally grow faster at first, as they become larger, they outperform white fir trees. At the extreme of their sizes, white fir out-performs red fir but these trees make up a very small proportion of the population in these scenarios. As

would also be expected, trees on more moist sites also out-performed drier sites. The value in simulations is that the moisture could be adjusted based on climate projections. The amount of moisture cannot be changed over time within the simulator but a range can be considered based on current and future moisture predictions.

A point of interest is that rounding errors could be contributing to the red fir advantage. White fir dominated stands and red fir dominated stands performed similarly for Tahoe when moisture variables were held constant, whereas red fir dominated scenarios out performed white fir dominated scenarios for Sequoia and Klamath. With further examination of the Tahoe stands, the white fir dominated stands grew faster than the red fir stands until the thin. The thin for red fir dominated stands induced a reduction of generally about 26% in terms of density, whereas the white fir stands experienced a thin of about 29% due to rounding errors (Table 39). The 3% difference could explain the change in dominance from white fir to red fir for the Tahoe scenarios. This also likely explains why the TWD scenario has such a long treatment persistence and red fir scenarios were better performers.

The most interesting scenario is SRD. It has the second shortest treatment persistence and the third greatest final density of the scenarios although it is a drier stand (Table 40). The shorter treatment persistence compared to white fir dominated stands is likely influenced by the difference in treatment density as mentioned above. Even after taking this into consideration, the scenario performance illustrates how well the red fir in Sequoia grow. The years sampled also had the lowest average April 1st snow pack

compared to the other two sites. The greater growth might be influenced by the trees being a different variety at each site. Similarly, the sites are far enough apart that substantial genetic differences in white fir are highly likely to also exist. This study is not comparing apples to apples in this regard; but assuming the category "SITE" keeps assumptions reasonable, this illustrates the value of healthy edaphic conditions. The red fir in the area in Sequoia studied have a history of large rings (G. Powell, pers. comm., 2013).

Conclusion

The greatest advantage of this simulator is that it is fairly intuitive for adjustments to be made by managers. The elevation can be changed by some truthing. The population can be adjusted based on stand inventories. The ingrowth and mortality functions can be adjusted by changing a few values or by eliminating them entirely and creating their own function in Visual Basic or populating them explicitly every five years. Thinning can also be tailored. For example, it can be modified to eliminate all red fir trees with high degrees of crown infection. The edge term is especially important because variable retention silviculture techniques are becoming more popular and group selection is a well-established technique. This is not a consideration that distance-independent simulators can account for directly.

Further research

Further research is needed in order to address the issues that made designing this stand growth workbook so difficult. First, individual trees maintain the same trajectory throughout their existence in the worksheet. The characteristics of level of damage and position, for both red and white fir and level of crown infection for red fir trees does not change as the trees grow. This cannot be adjusted for given this format since, if a tree were to move from one cell to another cell by subtracting a value in one cell and adding it to the next, the dimensions of the tree would change instantly to the dimensions of a tree in that new cell.

The mortality function is configured to eliminate the possibility of negative values occurring for distribution entries. Therefore, mortality is disproportionately assigned to healthy trees due to their higher proportion of occurrence and the way the mortality function operates. This may indirectly help to account for the likelihood that healthy trees might become less healthy over time but this project includes no data to support the transition of a tree from one category to another. Also, trees are not removed from the ingrowth diameter classes due to mortality because the mortality function is unable to accommodate this as presently constructed in this workbook. If this project is to be executed again, it is suggested that a different format be used. It should be one that could take into account the growth of each tree instead of grouping all trees of initial characteristics together.

The trees sampled had been targeted for sampling with the constraint that it was unlikely that they had been substantially disturbed within the past eight years. Therefore, with regard to treatment persistence, the assumption is made that trees that have been disturbed behave similarly to trees that have not been disturbed with similar characteristics and competition levels. This is a concern because both of these species exhibit root grafting as exhibited by living stumps. This makes root disease transmission likely and could possibly influence growth rates and increases in mortality after treatment. Time and treatments would have been the only way to validate this assumption, which was unreasonable for the timeframe and permissions granted.

Most importantly, it is necessary to replicate this study in order to validate the models. The values that were measured are not commonly available through publically available datasets, such as those produced by FIA In particular, CRN.INFECT, DAM.MOD, EDGE, and CR values measured in this study are not typically available. The way these terms were constructed is a convention of this study. The crown ratio measurement technique used here is unconventional since it takes the lowest branch into consideration instead of the average of the lowest branches. This may become a better recognized technique as Light Detection and Ranging (LiDAR) becomes more available since detecting the lowest branch of a tree is done more readily than detecting all of the branches and taking an average.

REFERENCES

Avery, T. E., & Burkhart, H. E. (2001). *Forest measurements 5th ed*. Boston, MA: McGraw Hill.

Barbour, M. G., Berg, N. H., Kittel, T. G. F., & Michael E. Kunz. (1991). Snowpack and the distribution of a major vegetation ecotone in the Sierra Nevada of California. *Journal of Biogeography*, 141–149.

Barbour, M. G., & Minnich, R. A. (1988). Califomian Upland Forests and Woodlands. *North American Terrestrial Vegetation*, 131–164.

Barbour, M. G., & Woodward, R. A. (1985). The Shasta red fir forest of California. *Canadian Journal of Forest Research*, *15*(3), 570–576.

Barry, W. J. (1971). *The ecology of Populus Tremuloides, a monographic approach*. University of California, Davis.

Beaty, R. M., & Taylor, A. H. (2001). Spatial and temporal variation of fire regimes in a mixed conifer forest landscape, Southern Cascades, California, USA. *Journal of Biogeography*, *28*(8), 955–966.

Bechtold, W. A., & Patterson, P. L. (2005). *The enhanced Forest Inventory and Analysis program—national sampling design and estimation procedures* (Gen. Tech. Rep. No. SRS-80) (p. 85). Southern Research Station, Asheville, NC: Forest Service, U.S. Department of Agriculture.

Chapin III, F. S., Margaret S. Torn, & Tateno, M. (1996). Principles of ecosystem sustainability. *American Naturalist*, 1016–1037.

Chappell, C. B., & Agee, J. K. (1996). Fire severity and tree seedling establishment in Abies magnifica forests, southern Cascades, Oregon. *Ecological Applications*, *6*(2), 628–640.

Clinton, B. D., Boring, L. R., & Swank, W. T. (1993). Canopy gap characteristics and drought influences in oak forests of the Coweeta Basin. *Ecology*, *74*(5), 1551–1558.

Cope, A. B. (1993). Abies magnifica. In *Fire Effects Information System, [Online]*. U.S. Department of Agriculture, Forest Service, Rocky Mountain Research Station, Fire Sciences Laboratory (Producer). Retrieved from http://www.fs.fed.us/database/feis/

Crookston, N. L., & Dixon, G. E. (2005). The forest vegetation simulator: A review of its structure, content, and applications. *Computers and Electronics in Agriculture*, *49*(1), 60–80. https://doi.org/10.1016/j.compag.2005.02.003

Das, A. (2012). The effect of size and competition on tree growth rate in old-growth coniferous forests. *Canadian Journal of Forest Research*, *42*(11), 1983–1995. https://doi.org/10.1139/x2012-142

Davidson, A. C., & Hinkley, D. V. (1997). *Bootstrap Methods and Their Applications*. Cambridge: Cambridge University Press.

Department of Water Resources. (n.d.). *California Data Exchange Center Historical Data Selector*. California. Retrieved from http://cdec.water.ca.gov/cgi-progs/selectQuery

Ernakovich, J. G., Hopping, K. A., Berdanier, A. B., Simpson, R. T., Kachergis, E. J., Steltzer, H., & Wallenstein, M. D. (2014). Predicted responses of arctic and alpine ecosystems to altered seasonality under climate change. *Global Change Biology*, *20*(10), 3256–3269.

Faraway, J. J. (2004). *Linear models with R* (1st ed.). CRC Press.

Fellows, A. W., & Goulden, M. L. (2008). Has fire suppression increased the amount of carbon stored in western U.S. forests? *Geophysical Research Letters*, *35*(12), L12404. https://doi.org/10.1029/2008GL033965

Fites-Kaufman, J. A., Rundel, P., Stephenson, N., & Weixelman, D. A. (2007). Montane and subalpine vegetation of the Sierra Nevada and Cascade ranges. *Terrestrial Vegetation of California. University of California Press, Berkeley*, 456–501.

Gesch, D. B. (2007). The National Elevation Dataset. In *Digital Elevation Model Technologies and Applications: The DEM Users Manual* (2nd ed., pp. 99–118). Bethesda, MD: American Society for Photogrammetry and Remote Sensing.

Gesch, D., Oimoen, M., Greenlee, S., Nelson, C., Steuck, M., & Tyler, D. (2002). The national elevation dataset. *Photogrammetric Engineering and Remote Sensing*, *68*(1), 5–32.

Griffin, J. R., & Critchfield, W. B. (1972). The distribution of forest trees in California., (PSW-82), 114 pp.

Hawksworth, F. G. (1977). *The 6-class dwarf mistletoe rating system* (Gen. Tech. Rep. No. RM-48) (p. 48). Rocky Mountain Forest and Range Experiment Station: Forest Service, U.S. Department of Agriculture.

Hodge, J. D. (1965). Variable Plot Cruising: A Short-Cut Slope Correction Method. *Journal of Forestry*, *63*(3), 176–180.

Keyser, C. E. (2008). Keyser, Chad E. comp. 2008 (revised November 2, 2015). Inland California and Southern Cascades (CA) Variant Overview – Forest Vegetation Simulator. Internal Rep. Fort Collins, CO: U. S. Department of Agriculture, Forest Service, Forest Management Service Center. 78p.

Koch, G. W., Sillett, S. C., Jennings, G. M., & Davis, S. D. (2004). The limits to tree height. *Nature*, *428*(6985), 851–854.

Laacke, R. J. (1990a). Abies concolor (Gord. & Glend.) Lindl. ex Hildebr. White fir. *Silvics of North America: 1. Conifers*, 36ą46.

Laacke, R. J. (1990b). Abies magnifica A. Murr., California red fir. *Silvics of North America*, *1*, 71–79.

Laacke, R. J., & Fiske, J. N. (1983). Red fir and white fir. *Agric. Handb*, *445*, 41–43.

Lanner, R. M. (1999). *Conifers of California.* Cachuma Press.

Lanner, R. M. (2010). Abies magnifica var. Critchfieldii, a New California Red Fir Variety from the Sierra Nevada. *Madroño*, *57*(2), 141–144. https://doi.org/10.3120/0024-9637-57.2.141

Liang, J., Buongiorno, J., & Monserud, R. A. (2004). *CalPro: A spreadsheet program for the management of California mixed-conifer stands* (Gen. Tech. Rep. No. PNW-GTR-619). Pacific Northwest Research Station: Forest Service, U.S. Department of Agriculture.

Maurer, E. P. (2007). Uncertainty in hydrologic impacts of climate change in the Sierra Nevada, California, under two emissions scenarios. *Cimatic Change*, *82*(3–4), 309–325.

Minnich, R. A. (2007). Climate, paleoclimate, and paleovegetation. *Terrestrial Vegetation of California*, 43–70.

Minore, D. (1979). Comparative autecological characteristics of northwestern tree species—a literature review., *PNW-GTR-087*. Retrieved from http://www.treesearch.fs.fed.us/pubs/25175

Monserud, R. A. (1984). Problems with site index: an opinionated review. In *Symposium Proceedings: Forest land classification: experiences, problems, perspectives*. Madison, Wis.: University of Wisconsin.

Mortenson, L. A. (2011). Spatial and ecological analysis of red fir decline in California using FIA data. Retrieved from http://ir.library.oregonstate.edu/xmlui/handle/1957/21828

Moser, J. W. (1976). Specification of density for the inverse J-shaped diameter distribution. *Forest Science*, *22*(2), 117–180.

Mote, M. (2006). Climate-driven variability and trends in mountain snowpack in western North America. *Journal of Climate*, *19*(23), 6209–6220.

Mutch, L. S., & Parsons, D. J. (1998). Mixed conifer forest mortality and establishment before and after prescribed fire in Sequoia National Park, California. *Forest Science*, *44.3*, 341–355.

Parker, A. J. (1982). The Topographic Relative Moisture Index: An Approach to Soil-Moisture Assessment in Mountain Terrain. *Physical Geography*, *3*(2), 160–168. https://doi.org/10.1080/02723646.1982.10642224

Reineke, L. H. (1938). *Perfecting a stand-density index for even-aged forests*. US Government Printing Office.

Ritchie, M. W. (1999). *A compendium of forest growth and yield simulators for the Pacific Coast states* (Gen. Tech. Rep. No. PSW-GTR-174) (p. 59). Albany CA: Pacific Southwest Research Station: Forest Service, U.S. Department of Agriculture.

Robinson, A. P., & Monserud, R. A. (2003). Criteria for comparing the adaptability of forest growth models. *Forest Ecology and Management*, *172*(1), 53–67. https://doi.org/10.1016/S0378-1127(02)00041-5

Shaw, J. D. (2005). Reineke's stand density index: where are we and where do we go from here. In *Proceedings: Society of American Foresters 2005 National Convention* (pp. 19–25). Retrieved from http://www.fs.fed.us/rm/pubs_other/rmrs_2006_shaw_j006.pdf

Skinner, C. N., & Taylor, A. H. (2006). Southern Cascades bioregion. In *Fire in California's Ecosystems* (pp. 195–224). Berkley: University of California Press.

Smith, D. M., Larson, B. C., Kelty, Matthew J., & Ahton, P. M. S. (1997). *The practice of silviculture: applied forest ecology* (9th ed.). John Wiley and Sons, Inc.

Soil Survey Staff. (n.d.). *Official Soil Series Descriptions*. Lincoln, NE: Natural Resources Conservation Service, United States Department of Agriculture. Retrieved from "http://soils.usda.gov/technical/classification/osd/index.html"

Stage, A. R. (1973). *Prognosis model for stand development* (For. Ser. Res. Pap. No. INT-137) (p. 32). Intermountain Forest & Range Experiment Station, Ogden, Utah: Forest Service, U.S. Department of Agriculture.

Stephens, S. L. (1998). Evaluation of the effects of silvicultural and fuels treatments on potential fire behaviour in Sierra Nevada mixed-conifer forests. *Forest Ecology and Management*, *105*(1–3), 21–35. https://doi.org/10.1016/S0378-1127(97)00293-4

Stephenson, N. L., Das, A. J., Condit, R., Russo, S. E., Baker, P. J., Beckman, N. G., … Alvarez, E. (2014). Rate of tree carbon accumulation increases continuously with tree size. *Nature*, *507*(7490), 90–93.

Sugihara, N. G., Van Wagtendonk, J. W., & Fites-Kaufman, J. (2006). Fire as an ecological process. *Fire in California's Ecosystems*, 58–74.

Taylor, A. H., & Skinner, C. N. (2003). Spatial patterns and controls on historical fire regimes and forest structure in the Klamath Mountains. *Ecological Applications*, *13*(3), 704–719.

Taylor, A. R., Chen, H. Y. H., & VanDamme, L. (2009). A Review of Forest Succession Models and Their Suitability for Forest Management Planning. *Forest Science*, *55*(1), 23–36.

Troyer, J., & Blackwell, J. A. (2004). *Sierra Nevada forest plan amendment: final supplemental environmental impact statement* (No. Vol. 46). Pacific Southwest Region: USDA Forest Service.

van Mantgem, P. J., & Stephenson, N. L. (2005). The accuracy of matrix population model projections for coniferous trees in the Sierra Nevada, California. *Journal of Ecology*, *93*(4), 737–747.

van Mantgem, P. J., Stephenson, N. L., Mutch, L. S., Johnson, V. G., Esperanza, A. M., & Parsons, D. J. (2003). Growth rate predicts mortality of Abies concolor in both burned and unburned stands. *Canadian Journal of Forest Research*, *33*(6), 1029–1038.

van Wagtendonk, J. W., & Fites-Kaufman, J. (2006). Sierra Nevada bioregion. *Fire in California's Ecosystems. University of California Press, Berkeley, California, USA*, 264–294.

Variable Plot Cruising: A Short-Cut Slope Correction Method: ingentaconnect. (n.d.). Retrieved August 5, 2014, from

http://www.ingentaconnect.com/content/saf/jof/1965/00000063/00000003/art00006

Venables, W. N., & Ripley, B. D. (2002). *Modern Applied Statistics with S* (Fourth). New York: Springer.

Warton, D. I., & Hui, F. K. (2011). The arcsine is asinine: the analysis of proportions in ecology. *Ecology*, *92*(1), 3–10.

Wensel, L. C., & Biging, G. S. (1988). The cactos system individual-tree growth simulation in the mixed conifer forests of California. *USDA Forest Service General Technical Report NC - North Central Forest Experiment Station (USA)*. Retrieved from http://agris.fao.org/agris-search/search.do?recordID=US8871950

Wensel, L. C., Meerschaert, W. J., & Biging, G. S. (1987). Tree height and diameter growth models for northern California conifers. *Hilgardia: A Journal of Agricultural Science (USA)*. Retrieved from http://agris.fao.org/agris-search/search.do?recordID=US8845130

Zouhar, K. (2001). Abies concolor. In *Fire Effects Information System, [Online]*. U.S. Department of Agriculture, Forest Service, Rocky Mountain Research Station, Fire Sciences Laboratory. Retrieved from http://www.fs.fed.us/database/feis/

APPENDIX

Definition of Terms

Angle gauge – a tool with a space which is used to identify whether a tree is in or out of a variable radius plot

ATSIXTY - the percent of mortality of DLTASDI the user chooses to occur, in terms of SDI units, at 60% of the maximum SDI

BA – Basal area measured at breast height

BAI – Basal area increment

BAL – Basal area attributed to trees larger than the target tree

Biltmore stick – a yardstick like device that assists in measuring DBH and height

BLC – the base of the live crown

CI – crown infection by cytospora canker

CR – Crown ratio (crown length/total height)

CUBE.BAI – the cube root transformation on the BAI response variable

DAM.MOD – the term that describes if a tree has more than moderate or less than moderate damage. The baseline is less than moderate.

DI – diameter increment

DBH – Diameter at breast height (1.4 m)

DCLASS - diameter class

DEM – Digital elevation model

DDist - the number of trees in a diameter class

DLTASDI - the amount SDI has increased over the past five years

EDGE.YN – binary term for edge or interior position of tree

GIS – Geographic information systems

GPS – Global positioning system

HT:DBH – height to diameter ratio

IGMAX - the maximum number of ingrowth trees

KNF – Klamath National Forest including Timber Products Company/Michigan-California Timber Company property

LAT.ADJ.ELEV – latitude adjusted elevation

Loupe – a small hand held magnifying glass without a handle

NED – National elevation dataset

RF.SDI – the proportion of the stand density index attributable to red fir

SDI – Stand density index

SDIL – Stand density index attributed to trees larger than the target tree

SDIINFL - the value, in SDI units, that represents the density for which the most trees would occur due to ingrowth.

SITE – term with levels KNF, SNF, and TNF

SNF – Sequoia National Forest

TNF – Tahoe National Forest

TPDfifteen - the initial number of trees in the 15 cm diameter class

TRMI.NO.DR – topographic relative moisture index used to estimate water availability at a location.

TRTTIME - the time since the last treatment

Wedge prism – a glass prism which helps determine which trees are in and out of a variable radius plot

WF.SDI – the proportion of the stand density index attributable to white fir